

Validation of Self-Healing Properties of Construction Materials through Nondestructive and Minimal Invasive Testing

Didier Snoeck, Fabian Malm, Veerle Cnudde, Christian U. Grosse, and Kim Van Tittelboom*

When studying the self-healing properties of construction materials, a plethora of destructive and nondestructive testing (NDT) techniques can be used. In this review, the applicability of different nondestructive test methods is discussed in detail. The methods can be categorized whether they are used to study the encapsulation and/or protection mechanism of the healing agent, the sequestered healing agent itself, the distribution of healing agents, the trigger mechanism for healing, the healing efficiency, or healing performance. Based on this categorization, nondestructive techniques found in literature are discussed. In this way, a robust understanding of the different techniques can be used for future research on self-healing construction materials.

Although it is necessary, such repair or maintenance works cannot always be performed due to a lack of time, resources, or accessibility. The cracks need to be repaired somehow as the durability of the element and construction may be endangered. Self-healing is one of the promising techniques which can be used.^[6]

A self-healing process can be defined as an autonomous (or with limited human intervention) in situ repair of damage occurring to materials. Up to a certain extent, some building materials own a natural self-healing capacity, which contributes to their durability.^[6–19] The natural

self-healing ability of building materials such as lime mortar, cementitious materials, and even natural stone is related to fluid flow migration.^[7] Water, intruding the porous building materials due to capillary uptake or water infiltration, allows the dissolution of calcium bearing compounds present in the building material. The fluid transports them, from a zone rich in calcium, to voids and cracks, where precipitation of the calcium occurs. These recrystallized calcium compounds may fill small cracks or close open pore networks. This type of self-healing process is a natural and spontaneous process, and not the result of special design features.^[7] However, as the natural self-healing capacity of construction materials is limited, a lot of work has been done to develop building materials with increased or controlled self-healing properties. For a comprehensive review on self-healing mechanisms in construction materials, we refer to the first papers in this Special Issue of Advanced Materials Interfaces.

1. Introduction


1.1. Cracking in Construction Materials and Self-Healing as a Possible Solution

The disadvantage of some construction materials such as concrete and asphalt is that they are prone to cracking. This cracking is caused by shrinkage, freezing, and thawing, exposure to aggressive agents such as sulfates and salts, differential settlements, thermal actions, mechanical loading, among others.^[1–5] Maintaining construction elements and thus the material itself is needed and repair works are imminent.

Dr. D. Snoeck, Prof. K. Van Tittelboom
Magnel Laboratory for Concrete Research
Department of Structural Engineering
Faculty of Engineering and Architecture
Ghent University
Tech Lane Ghent Science Park, Campus A
Technologiepark Zwijnaarde 904, B-9052 Ghent, Belgium
E-mail: Kim.VanTittelboom@UGent.be

F. Malm, Prof. C. U. Grosse
Center for Building Materials
Chair of Non-Destructive Testing
Technical University of Munich
Baumbachstrasse 7, D-81245 Munich, Germany

Prof. V. Cnudde
PProGRes-UGCT
Department of Geology
Faculty of Sciences
Ghent University
Campus Sterre, Krijgslaan 281, Building S8, B-9000 Ghent, Belgium

 The ORCID identification number(s) for the author(s) of this article can be found under <https://doi.org/10.1002/admi.201800179>.

1.2. The Use of Nondestructive and Minimal Invasive Techniques to Study Self-Healing

When studying the self-healing properties of construction materials, different destructive and nondestructive testing (NDT) techniques can be used.^[13,20] The methods can be categorized based on the fact whether they are used to study the mechanism to encapsulate or protect the healing agent, the properties of the sequestered healing agent, the distribution of the healing mechanism, triggering of the healing mechanism, and the healing efficiency or healing performance. Based on this differentiation, multiple nondestructive and minimal invasive testing techniques are discussed in this review paper (see Sections 2–7). Most of them have the obvious advantage that the specimen or

DOI: 10.1002/admi.201800179

component is not damaged during inspection. So, the specimen or component remains available for further testing, what is not the case when destructive test methods are used.

Mostly, crack formation is required to activate the healing process. One needs to mention that the cracking technique itself is of destructive nature. The evolution of cracking and crack healing can then be monitored and studied over time by means of nondestructive testing. Although several nondestructive characterization techniques exist, it remains important to mention that they often require a sampling strategy and sample preparation and therefore indirectly interfere with the original construction material. In most cases, however, it is possible to keep such a process minimal invasive for the material.

1.3. Microscopic Investigation and Electron-Based Techniques to Study Self-Healing

Generally, visual inspection techniques are among the most-used nondestructive techniques including optical microscopic analysis, which requires samples on the order of a few centimeters. A frequently used microscopic technique uses polarized light to visualize the studied object in transmission to characterize minerals and structures.^[21] This object can range from the building material itself to the healing agent or product. The preparation of a thin section is mostly considered to be a destructive technique as the material is cut to a small slice and as it is impregnated with epoxy resin.^[22] This technique is thus not discussed within this review paper. However, optical, digital, and/or stereo microscopic analysis is one of the considered nondestructive measurement techniques. A plethora of research studies report on the use of these testing methods, which will be discussed in the following sections of this review paper.

Next to optical microscopy, an analogous technique has proven to be useful to study the properties on a micro- and nanoscale, using electrons. Since electrons can be accelerated up to a velocity very close to the speed of light, it is possible to create electrons with a wavelength down to 0.1 nm, enabling scientists to go down to the atomic and molecular scale of matter. A scanning electron microscope or SEM is a type of electron microscope that images a sample by scanning it with a high-energy beam of electrons in a raster scan pattern. By using a focused beam of electrons, the SEM reveals levels of detail and complexity inaccessible by optical microscopy. The electrons interact with the atoms of the sample, producing signals that contain information about the sample's surface topography, composition, and other properties such as electrical conductivity. In the most common or standard detection mode, secondary electron imaging or SEI, the SEM can produce very high-resolution images of a sample surface, revealing details about less than 1–5 nm in size.^[23] In order to obtain SEI images, the samples need to be dry and coated with gold or carbon (in order to be electrically conductive) and an SEI detector needs to be present. Often, a back-scattered electron (BSE) detector is used in analytical SEM along with the spectra made from the characteristic X-rays.^[24] Because the intensity of the BSE signal is strongly related to the atomic number (*Z*) of the specimen, BSE images can provide information about the distribution of different elements in the sample, while energy-dispersive X-ray spectroscopy (EDS or EDX)^[20,22] is



Didier Snoeck is a postdoctoral research fellow of the Research Foundation Flanders (FWO) at the Magnel Laboratory for Concrete Research of Ghent University, Belgium. He is a member of RILEM and active in several technical committees. The main topics of his research are superabsorbent polymers, concrete technology, durability, nano- and microstructural properties, self-sealing, and self-healing of cementitious materials.



Fabian Malm studied civil engineering at the Technical University of Munich (TUM), Germany. Since 2013 he has been working as a research assistant at the Chair of Non-Destructive Testing at TUM. In addition to teaching activities, his research topics include nondestructive testing of damage mechanisms in different materials, setting of fresh concrete, and self-healing of cementitious materials.



Kim Van Tittelboom is a professor in the field of Structural Engineering at Ghent University (Faculty of Engineering and Architecture, Department of Structural Engineering). She is MC substitute in COST CA15202 SARCOS and active member of RILEM TC DFC and TC SHE. Her research interests focus on sustainable structural engineering through self-healing of cracks in concrete, preventing reinforcement corrosion, and 3D printing of cementitious materials.

commonly used to perform an elemental analysis or a chemical characterization of a sample based on its unique atomic structure determining a set of peaks on its electromagnetic emission spectrum. EDS is one of the variants of X-ray fluorescence spectroscopy which relies on the investigation of a sample through interactions between electromagnetic radiation and matter, analyzing X-rays emitted by the matter in response to being hit with charged particles. Its characterization capabilities are due in large part to the fundamental principle that each element has a unique atomic structure allowing X-rays—that are characteristic

of an element's atomic structure—to be identified uniquely from one another. By means of EDX it is possible to perform point analysis, line scans, and point mappings.^[25] Mostly, Rietveld analysis is needed to obtain quantitative results.

1.4. Use of X-Ray or Neutron Radiography and/or Tomography to Study Self-Healing

Microscopy has always been an intriguing area of science since it allows looking at objects in a way which is beyond the possibilities of the naked eye. Although modern optical microscopes make it possible to look at matter at the microscopic scale, there is also a limit: the wavelength of visual light. The smallest distinguishable features are determined by this wavelength due to the fact that even a microscope with perfect lenses is subjected to diffractive effects. By changing the source of illumination to a radiation probe with a smaller wavelength, smaller details can be observed and, as mentioned before, the electrons used as probe in electron microscopes can reach resolutions up to the nanometer scale. One issue, which is common to both microscopic techniques, light microscopy, and electron microscopy, is the need for sample preparation. Although it is possible to study objects by detecting reflected light/particles, even then some kind of sample preparation (like polishing) is often needed. Moreover, in both modes, no true 3D information could be obtained (only slices or surfaces are visualized). While minimal invasive imaging techniques such as electron microscopy and fluorescence microscopy can be used to study the self-healing effect, these methods have the drawback that identical locations cannot be visualized before and after healing. Therefore, nondestructive imaging techniques are preferred as they allow to monitor the dynamic changes in real time. Several nondestructive imaging techniques, such as X-ray radiography, neutron radiography, X-ray computed tomography (X-ray CT), neutron CT, among others, have been used to study self-healing of building materials at both qualitative and quantitative levels.

An important fact about X-rays, next to the fact that their resolution is higher than that of light, is that their penetrating power is largely dependent on their energy (which is directly related to their wavelength), making it possible to adjust the energy of the source to the type of sample under investigation (based on size, composition, among others). This makes X-rays not only suitable for microscopic purposes, but in general provides a method for nondestructive imaging of objects of all sizes (from several meters large down to only a few micrometers).^[26,27] X-ray radiography and computed tomography provide nondestructive 2D and 3D visualization and characterization, creating images that map the variation of X-ray parameters like attenuation within objects. An X-ray beam is attenuated when X-ray photons are removed from the beam by interaction with matter. Most transmission CT devices are based on the principle that the object is positioned in between an X-ray source and an X-ray detector. CT scanning in material science requires a rotational motion of the sample relative to the source–detector system. While for medical scanners the object remains fixed and the X-ray source and detector revolve around the sample, in CT analysis the object is mostly placed on a rotation platform with a fixed X-ray source and detector. Modern

X-ray detector systems are often based on 2D-pixel arrays such as CCD cameras, flat-panel detectors, or image intensifiers. They measure X-ray transmission in the form of digital radiographs that are stored on a hard disk. Hundreds of X-ray radiographs are acquired for one single X-ray CT scan from different rotation angles between 0° and 360°. After the data collection, reconstruction algorithms calculate the slices or cross-sections through the object. The smaller the sample, the better the resolution of the images will be. X-ray CT is ideal to characterize nondestructively the internal 3D structure of a construction material. Therefore, this technique has often been used to characterize the self-healing properties of a material.

When dealing with natural self-healing in construction materials, this is mostly linked to a high water supply and the possibility to dry as during cycles of wetting and drying ions can be mobilized. Small amounts of water inside a stone are sometimes difficult to detect using X-rays and then well-known techniques to visualize water inside a building material are neutron radiography and tomography. Neutron imaging is a radiographic imaging method using neutrons. As such, the approach is rather similar to X-ray imaging as neutrons are also able to penetrate material depending on the specific attenuation properties of that material. Using neutrons, it is also possible to obtain the 2D or 3D internal structure of the object under investigation as neutron radiography and CT, similarly to X-ray radiography and CT, use radiographic projection images of the sample. For neutron CT, radiographs are required at different angles (typically either 180° or 360° to cover the whole sample). After reconstruction of the stack of radiographs, a 3D image of an object is created by combining multiple planar images with a known separation just like for X-ray CT.

Both X-ray CT and neutron CT have their pros and cons. While X-rays mainly interact with the electrons of an atom, neutrons rather interact with the atomic nucleus. Because of their different radiation matter interaction characteristic, there is a higher probability for X-ray interaction with atoms with a higher atomic number, while neutron interaction can lead to a good visualization of water because of the high scattering probability with the hydrogen atom, having a low atomic number. However, neutrons can also initiate the activation of the nuclei by neutron capture, producing instable radioactive isotopes. Therefore, samples need to be tested for radioactivity after neutron imaging. Besides a different linear attenuation coefficient between X-rays and neutrons, they also can reach different resolutions. X-ray sources as well as synchrotron radiation sources can reach easily a resolution below 1 μm. Additionally, synchrotron radiation sources have a very high brightness. On the contrary, neutron sources comparably have a lower source brightness and cannot easily be focused. Typically, neutron CT imaging is on the order of 10 μm and above. On the other hand, neutron CT imaging is ideal if one wants to look inside a dense rock sample of several centimeters toward water migration as the rock will become almost invisible for neutrons while the water is clearly visualized.

1.5. Acoustic Techniques to Monitor Healing

Based on the propagation of elastic waves in solid media, ultrasonic testing can be applied to study material properties or

material changes due to mechanical, thermal, and chemical effects. Elastic waves are mechanical expansion/elongation processes, characterized by temporal and spatial expansion.^[28–30] In solids, elastic waves can propagate in different modes. The most important are the two body waves—the longitudinal (or compression) waves with particle motions in the direction of wave propagation and the transverse (or shear) waves, with particle motion perpendicular to the direction of propagation.^[31] In a homogeneous half-space, the surface waves like Rayleigh waves are produced by the interference of longitudinal and transversal waves with the boundary. Rayleigh waves appear in an elliptic retrograde motion. The other types of surface waves, i.e., Love waves, occur only in layered media. In solids with dimensions smaller than the wavelength or with interfaces in the wave direction, Lamb waves and torsional waves can be generated. In finite media, i.e., specimens with boundaries, the direct waves with modes as mentioned above (compressional, shear, Rayleigh, Love, and Lamb waves) are followed by waves that are summarized as “coda.” The coda waves are caused by reflections, mode conversions, and other effects, and contain a more or less “diffused wave field”^[32] as well as information about material properties. In ultrasonic testing, elastic waves with frequencies between 20 kHz and 10 MHz are typically used. In this way, various measuring and data processing techniques are implemented depending on the objective and the actual boundary conditions.

The position of the transmitting and receiving sensors defines the measurement procedure. An ultrasonic measurement in transmission is based on the propagation of an elastic wave which is induced at a certain point A and recorded at another point B, while A and B are typically at opposite sides. In comparison, the pulse echo technique is based on the reflection of the excited ultrasonic pulse and sensors A and B typically coupled to the same side of the specimen. Depending on the frequencies of the ultrasonic wave, reflections and mode conversions, a coherent or an additional incoherent (diffuse) field has to be taken into account. A concrete test specimen can be considered as homogeneous if the wavelength of the considered ultrasonic waves is larger than its aggregates. At frequencies where the wavelength and the aggregate or other internal features (pore size) are of the same order, waves are highly attenuated by scattering and dissipation.

In time domain, the velocity of the ultrasonic signals (derived out of the “time of flight”) is an important parameter of the signal.^[33–37] Other useful information for the characterization or monitoring of concrete structures, mainly based on coda waves, can be provided by the amplitude^[38–40] or energy of the full signal^[41–44] waveform in terms of coda wave interferometry.^[45–49] A transformation into the frequency domain can give further insight^[42,50,51] into material properties. Several studies proved that even small changes in the material microstructure are detectable using coda-wave interferometry techniques. However, it is important to know that the above-mentioned ultrasonic analysis methods or parameters are highly sensitive to the measurement setup. A good way to analyze the impact of the setup is considering the NDT application as a measuring chain, where all the individual elements have an influence on the resulting data. Following system theory,^[52,53] individual transfer functions of test setups and the components of the measuring chain (sensor characteristic, coupling, cable,

A/D converter, etc.) can be determined. After quantifying (and eliminating) these influences from the signal, material properties such as composition, curing conditions, moisture content or microstructure effects like pores as well as the mixing process of cementitious materials can further have an impact on the transmitted and received signals device.^[54]

Compared to individual ultrasound measurements conducted once or a few times in a nonrepetitive way, ultrasonic testing methods can also be applied in a more or less continuous way. Ultrasonic transmission measurements have been used to monitor the setting behavior of fresh mortar or concrete.^[55–61] This application also enabled an in situ evaluation of the polymer-based healing process in cementitious materials.^[62] In addition, different modifications of the transducer setup can be found in the literature.^[63] In comparison to constant ultrasonic measurements, burst signals are primarily used to increase the measuring frequency. This restricts the data analysis technically in a considerable way. Due to requirements of wave attenuation (pulse energy) and frequency evaluations (broad frequency band), such measurements are demanding concerning sensors and the electronic equipment such as amplifiers. Since the control of crack formation is usually carried out under high load, e.g., in a three-point bending testing machine, interferences of the measured signals with low amplitudes with electronic noise from the machines can have an effect on the data quality. This involves, for example, low-frequency vibrations or electromagnetic interference. Noise should be reduced as far as possible in advance and taken into account in the measurement records. Filtering or postsignal processing are suitable tools to extract relevant information from the recorded noisy signals.^[53,64–67] With regard to the application of ultrasonic-based methods for the evaluation of self-healing effects in cementitious materials Ahn et al.^[68] are giving an overview.

Impact resonance and vibration analysis are applied to determine the elastic material properties of mortar and concrete test specimens. By evaluating the resonance frequencies and the eigenfrequencies of the specimen, taking the given geometry into account, this nondestructive technique allows to derive global information about the structural damage conditions by changes of the natural frequencies or their amplitudes. Providing that a certain solid media behaves ideally elastic and is homogenous and isotropic, the dynamic modulus of elasticity (Young’s modulus) of a cementitious material is mainly related to its dimensions, elastic material constants, and density. Therefore, the elastic and also the shear modulus of an object can be calculated from the measurement of the fundamental longitudinal, flexural (transverse), and torsional frequencies and the corresponding mathematical relationship^[69,70]—a feature that is well established in scientific research and material testing.^[71–75] Material changes due to physical and chemical stresses are detectable by the change of the natural frequencies of the entire system.

Elastic waves, which are emitted in concrete during crack propagation for example under mechanical or thermal load, are referred to as acoustic emissions. In acoustic emission (AE) analysis, the waves are received by suitable sensors on the surface of the structure and transmitted as a transient analog signal. A transient acoustic emission signal is composed of many individual frequencies of different wavelengths while these frequencies are governed by fracture parameters such

as crack width and length.^[76] The typically considered frequency range of acoustic emissions in concrete structures is between 20 and 100 kHz.^[77] Signals are recorded and evaluated in the ultrasonic frequency range due to ambient noise conditions and have a low signal amplitude compared to ultrasonic methods. The AE signal amplitudes have to be amplified accordingly before recording.^[31] If the displacement measured by an AE sensor is not absolutely calibrated, AE data are typically relative values and the comparison of different individual experiments and setups is difficult. AE analysis detects irreversible deformations and is therefore suitable for the analysis of temporal-spatial crack propagation in both the outer and inner regions of structures in real time, e.g., for permanent monitoring of bridges.^[77]

There are generally two different ways to record and analyze AE signals. Using a more qualitative parameter-based way, parameters such as crossing a given threshold, maximum amplitude, rise-time or signal duration are extracted from the transient signal and stored.^[77] This enables for a fast and widely automatic data processing but the individual signal is not recorded. A subsequent verification of the results and in particular a discrimination between signal and noise is impossible. A more quantitative, i.e., signal-based, way of AE analysis is made possible through the recent improvements in the field of electronics and computation (data processing, storage, and memory capacities). Here, in contrast to the qualitative analysis, the complete signal is recorded and stored, which allows for both a detailed analysis and a subsequent review.^[31] The signal-based method of AE analysis is based on the localization of the acoustic emissions by proper algorithms similar to seismology and the hypocenter localizations of earthquakes. To localize an AE event, different algorithms can be used. Most of them are based on the triangulation method (Geiger method in seismology) or the Bancroft algorithm^[78] (developed for the Global Positioning System), but there are many modifications and some new algorithms defined.^[79–85] The classic 3D localization of the acoustic emissions is based on the relative difference of the travel times from the source to the individual sensors and is defined by the onset time of the P-wave (or other wave modes) at the individual sensors. In order to determine the location of the source in three dimensions a minimum of four determined arrival times are required to calculate the four unknowns (three Cartesian coordinates and source time). It is important to ensure good spatial coverage of the AE sources using a sufficient number of sensors. In practice, a number of sensors significantly larger than four are required to increase the reliability of the localization derivations and to enable for numerical accuracy calculation. Considering the full waveform of AE signals provides a tool to evaluate the fracture mechanical processes in the material. This refers to the stresses in the fracture zone, the failure mechanisms (modes I, II or III), and the forces around the crack.

1.6. Purpose of This Review Paper

Multiple of the aforementioned nondestructive and minimal invasive testing techniques has been applied to study self-healing in construction materials. In the following sections,

these techniques are categorized and discussed on their use to study self-healing characteristics. At the end of this paper, a summarizing table shows the possibilities, boundary conditions, and advantages and disadvantages of the nondestructive techniques which can be used.

2. Techniques to Study the Encapsulation and/or Protection Mechanism of the Healing Agent

Some healing agents need to be encapsulated or protected from the surrounding matrix. Of course, one needs to be certain of the effectiveness of such encapsulation or protection technique. Different nondestructive and minimal invasive test methods can be applied and are thoroughly discussed below.

2.1. Performance and Physical Properties of Capsules and Protection Materials

The most easy and quick analysis is by naked eye or microscopic analysis for example of protection techniques for superabsorbent polymers (SAPs) used to promote autogenous healing in cementitious materials.^[86] As the incorporation of SAPs can be detrimental for the mechanical properties of a cementitious material with a high water-to-binder ratio due to macropore formation upon absorption of mixing water,^[87–89] a solution may be that the SAPs may be either pH responsive^[90,91] or may be coated.^[92] In low water-to-binder ratio systems, the SAPs may have a positive influence in terms of mechanical properties due to internal curing.^[88] The coating could be studied microscopically or by means of filtration tests. In these tests, water is added to the coated SAP and it is investigated whether the coating is able to slow down the absorption of mixing water.^[92] Also to study the performance of encapsulated healing agents, microscopic analysis has been used. In the study of Wang et al.^[93] the effectiveness of encapsulating a bacterial healing agent to heal cracks in cementitious materials was investigated by microscopy.^[93]

Currently, the effective contact angles inside a pore system can also be measured. Armstrong et al.^[94] directly determined the curvature of a fluid interface of a brine in a sandstone in order to calculate the capillary pressure through direct pore-scale imaging. Andrew et al.^[95] and Schmatz et al.^[96] measured the contact angle directly using broad ion beam-scanning electron microscopy (BIB-SEM) and micro-CT. Klise et al.^[97] developed a method to automatically record contact angles from large images. In the past, this direct approach has been successfully applied to predict fluid behavior inside porous materials, such as rocks^[98] and could also be a tool in the framework of characterizing self-healing.

Contact angle measurements have been used by Van Tittelboom^[99] to compare the release efficiency of a polyurethane based healing agent, used for crack healing in cementitious materials, from glass capsules and ceramic capsules. Therefore, the surface energy of glass, ceramic, and polyurethane was calculated based on these contact angle measurements. While the measured surface energy of ceramic was lower than the total surface energy measured for polyurethane, the value measured for glass approached the one for polyurethane. This led to the conclusion

that ceramic capsules have a lower capacity to be moistened by polyurethane and would thus result in a higher release efficiency. Contact angle measurements together with microscopic analysis may also show the functionalization of microcapsules induced by sunlight.^[100] If a change in surface property such as higher hydrophobicity or hydrophilicity is predicted, this technique can quickly show whether healing can occur.

2.2. Size, Size Distribution, Individuality, and Morphology of Encapsulation Materials

Visual observation, optical microscopy analysis, and SEM analysis can be useful techniques to study the size and the size distribution of (micro-) capsules.^[101–104] Larger capsules can be microscopically studied whereas the smaller capsules should be studied with SEM analysis. While some researchers tend to obtain a uniform capsule size distribution, others are in favor of a grade of capsule diameters. As there would be a correlation between the rupture force and the particle size of microcapsules, Lv et al.^[103,105] applied microcapsules with different grade of diameters (obtained by sieving) allowing their self-healing system to respond to varying trigger forces and thus to heal cracks of different crack widths (see also Section 5.2).

To obtain a homogenous distribution of the capsules inside the matrix (see Section 4), it is important that the (micro-) capsules do not stick together. Lv et al.^[103] used optical microscopy to show that their phenyl formaldehyde resin microcapsules are separated from each other and would not agglomerate inside a concrete matrix. Also Su et al.^[104] made use of SEM analysis to prove that their melamine formaldehyde microcapsules with rejuvenator only adhere to a limited extent and would thus not agglomerate inside an asphalt matrix.

SEM is also an ideally suited technique to study the morphology and the surface of microcapsules. Liao et al.^[106] and Su et al.^[107] determined the microcapsule size, shell morphology, and shell thickness using SEM. Lv et al.^[103] used SEM to show that their developed polymeric microcapsules with phenyl formaldehyde resin shell have a regular globe shape and a smooth surface. Also Dong et al.^[101] used SEM to show that their ethyl cellulose capsules had a spherical shape. The capsules of Lv et al.^[103] and Dong et al.^[101] were prepared for embedment in cementitious self-healing materials, but also when capsules are meant to be embedded in self-healing asphalt, SEM has been applied by Su et al.^[104] to study the surface morphology of their melamine formaldehyde capsules containing rejuvenator. As the mixing process may have a big impact on the capsule morphology, Dong et al.^[101] studied the shape of the capsules again after mixing by optical microscopy. Lv et al.^[103] used X-ray CT to prove that their phenyl formaldehyde resin microcapsules survived the mechanical mixing during sample preparation. In an earlier study of Dong et al.,^[108] the morphology and the surface of their urea formaldehyde microcapsules were investigated with optical microscopy. Moreover, the morphology of the capsules was studied at different synthesis stages showing the improvement obtained for each of the steps. After complete capsule synthesis, deposits of polyurea formaldehyde particles were noticed at the surface, which would increase the roughness and the bond of the capsules with the cementitious matrix.

Additional information with regard to the capsules can be gained from an SEM analysis when broken capsules are investigated. The capsule wall thickness can be measured and the homogeneity of the wall thickness can be investigated. In the study of Lv et al.^[103] and Su et al.,^[104] this information was used to obtain an idea about the ratio between the shell thickness and the diameter of the capsules and thus to have an idea about the capsules storage capacity.

2.3. Fracture Behavior of Encapsulation Materials

If crack formation is used to trigger the healing mechanism (see Section 5), capsules should break and release their content when being crossed by a crack. SEM was used by Lv et al.^[103] to study the rupture pattern of their microcapsules and allowed them to conclude that their capsules had a brittle fracture behavior. In addition, Lv et al.^[103] used optical microscopy to study the fracture behavior of their microcapsules before and after being embedded in a cementitious matrix. First, they studied the microcapsules being placed between two glass plates with optical microscopy. It was shown that the capsules were broken when compression was applied on the glass plates. Analyzing the fracture plane of a cementitious matrix with embedded capsules by optical microscopy also showed fracture of the capsules and showed that the capsule walls remained embedded in the cementitious matrix, so it could be concluded that there was a good bond between the capsule wall and the matrix.

2.4. Stability and Durability of Encapsulation Materials

The stability and durability of capsules is also a major issue, which needs to be investigated. When capsules need to be embedded inside a concrete matrix, they are exposed to a very harsh, alkaline environment with a pH ranging from 12 to 13. SEM is one of the techniques, which can be used to investigate whether the capsules can withstand this harsh environment. In the study of Lv et al.^[103] phenyl formaldehyde resin microcapsules were exposed to a simulated concrete pore solution for 48 h and subjected to an SEM analysis after rinsing with deionized water. It was shown that the shape of the capsules maintained but that the surface was covered with some granular substance, which was believed to be a layer of deposited calcium carbonate which had no negative effect on the capsules. When capsules need to be embedded inside an asphalt matrix, they need to withstand both the mixing procedure and the exposure to thermal cycles. Su et al.^[104] tested the integrity of their melamine formaldehyde microcapsules by optical microscopy after exposure to heating and squeezing.

2.5. Parametric Analysis of Encapsulation Techniques

Mostavi et al.^[109] used SEM analysis to perform a parametric study and select the most ideal preparation parameters for the production of their double-walled polyurethane /urea-formaldehyde microcapsules containing sodium silicate for healing cracks in concrete. The influence of the agitation rate, pH and

temperature on the shell thickness, and size and morphology of the prepared capsules were characterized using SEM to determine the optimum production process. It was concluded that increasing the agitation rate resulted in better spherical formation of the microcapsules, lower pH values resulted in less cracking of the capsule shell and more complete shell formation, and it was also shown that increased temperatures decrease the density of pores on the microcapsule surface.

3. Techniques to Study the Sequestered Healing Agent

Prior to adding a healing agent into a construction material and prior to healing, the performance of the healing agent needs to be studied. In this way, one gets a first indication whether the healing agent will result in successful crack healing within the construction material.

3.1. Visual Observation of the Healing Agent

In cementitious materials, many healing agents can be used. Microscopic analysis has been applied to study microcapsules containing different healing agents,^[100,110–114] expansive agents and crystalline products,^[115,116] synthetic microfibers,^[86,117–120] steel fibers,^[121] superabsorbent polymers,^[22,86,122–125] bacterial spores,^[126,127] among others. Microscopic analysis is used to determine the size and the morphology of the healing agents. In this way, information about the surface of the materials can be found. Also the type of fiber and shape can be interesting to study as the form may lead to a different cracking behavior and healing.^[122,128]

The porous nature and porosity of natural fibers for strain-hardening cementitious materials aiming at autogenous healing can be investigated using microscopy.^[129–132] In this way, the authors know which effects and water absorption could be expected, as the fibers may partially absorb mixing water, leading to an unwanted reduction in workability. The microscopic technique can also be used to verify spore formation in an easy way.^[127] Growth of cells could easily be visualized by increased turbidity of the medium. For the SAP healing system, not only the visual appearance of an SAP particle can be studied, also their 3D distribution can be investigated,^[123,125,133] and their swelling ability as a function of time by dropwise addition of water can be determined.^[86,122] By subsequent image analysis, the swelling capacity can also be estimated based on volume increases.^[86,134]

3.2. Microscale and Elemental Composition of the Healing Agent

SEM combined with EDX spectroscopy is a commonly used technique to study the properties of a healing agent on a microscale. The technique may also be used to study the morphology, size, and shape of the healing agents. Compared to microscopic analysis, SEM enables to study the bacteria at nanometer to micrometer scale.^[127] It allows determining the shape and size of the bacteria. Carriers for immobilizing bacteria can

be studied as well by means of SEM and EDX analyses,^[126] showing whether or not bacteria are present within the carrier and in which number they are present. Furthermore, the polymerization technique and the porosity of SAPs can be studied in detail by SEM analysis.^[122,135] This allows estimating the swelling characteristics and amount of swelling as it is influenced by the specific surface area of the SAP exposed to the used liquid. Furthermore, powdery expansive agents and crystalline admixtures can be studied and characterized, prior to mixing into a cementitious material.^[136] By using SEM, the irregular shape and size range of the crystalline agents could be studied. Furthermore, EDX analysis can be used to study the constituents of the crystalline admixtures.

3.3. Stability of the Healing Agent

In studies with regard to bacterial self-healing in cementitious materials, the viability of bacteria can be tested beforehand, prior to healing in situ and next to the already mentioned microscopic analysis. The crystallization by means of bacteria can be studied by means of SEM, CT, X-ray diffraction (XRD), and thermogravimetric analysis (TGA) on the obtained material.^[137–139] In this way, one can be certain whether or not the bacteria are able to precipitate the wanted crystals, when exposed to similar environmental conditions as compared to the application in the construction material. Other healing agents which can be studied by means of TGA are for example SAPs^[122] and MgO type of expansive agents,^[140] among others. TGA is a technique where a small amount of material is heated while recording the mass loss. Based on the mass loss, the composition of the material can be investigated and it can be determined whether a material would degrade at certain temperatures. If some healing agents would be exposed to very high temperature conditions, they may start to degrade or dissolve, which is unwanted.

As mentioned in Section 2, Lv et al.^[103] studied the stability of their microcapsules in a concrete pore solution by SEM analysis. In addition, the availability and the status of the encapsulated healing agent were investigated after immersion of the capsules in a simulated concrete pore solution. After immersion, capsules were ruptured by compression and investigated by an optical microscope proving the presence of healing agent in the capsule core. This led to the conclusion that the concrete pore solution had limited effect on both the capsule wall and the healing agent.

3.4. Leakage Properties of the Healing Agent

Lv et al.^[103] also used optical microscopy to investigate whether the DCPD healing agent embedded in the phenyl formaldehyde resin microcapsules is released upon capsule breakage. When the capsules were broken between two glass plates, release of the healing agent was noticed. Also when capsules were embedded in a cementitious matrix, release of the healing agent was noticed when studying a crack plane by optical microscopy. However, it should be noticed that during this experiment Lv et al.^[103] heated their samples until 30 °C

to speed up the release of healing agent. As this heating may have a major effect on the viscosity of the healing agent, it will favor the leakage efficiency of the agent (and not only speed up the release).

Gilbert et al.^[141,142] performed experiments in which the outflow of the two components of a polyurethane-based healing agent (each of them with its own viscosity) was investigated within concrete cubes, with an artificial flat crack with a width of 300 μm , while scanning with X-rays. Based on the concept of differential imaging, two scans were made per experiment: one before the glass capsules containing the healing agent was broken and one after. Prior to breakage of the glass capsules (Figure 1a), 3D image analyses were performed to quantify the volume of healing agent inside the capsules from the reconstructed CT images. After breaking the glass capsules by a slight tap on the smallest concrete prism, part of the healing agent leaked out of the capsules, and more than half stayed behind in the parts of the capillaries furthest removed from the crack (Figure 1b). However, only a small volume of healing agent was found in the gap between the concrete blocks (Figure 1c), which primarily was linked to one component of the healing agent. For one of both components the viscosity seemed to be too low, which resulted in the fact that it did not stay in the gap but was absorbed by the matrix (a result that could visually be confirmed after the test). Since concrete is known to have a wide pore size distribution, it is not unlikely that part of this component had to be found in pores with a size smaller than the resolution of the X-ray scans (typically on the order of micrometers) leaving this component therefore undetectable on the CT scans. It could thus be concluded that if the viscosity of the healing agent is too low, it is absorbed by the matrix. However, also from the second component only part could be found in the crack. This is caused by the fact that if the crack is formed in a sudden way (in this study impact

loading was applied) and if the crack is too wide (in this case the crack width amounted to 300 μm) the healing agent will not flow out of the capsules as the capillary effect in the glass capsules retains the fluid inside.

Also in one of their later studies,^[143] this research group made use of X-ray CT to visualize leakage of the healing agent. This time, scanning was performed on cores drilled from large concrete beams, to prove that a later used one component polyurethane leaked out of the glass capsules and flew into realistic cracks made in a large concrete beam (150 mm \times 250 mm \times 3000 mm) loaded until an average crack width of 250 μm during a four-point bending test.

4. Techniques to Study the Distribution

When adding certain healing agents to construction materials, they may clog together. However, a nice dispersion is wanted and the self-healing mechanism should be uniformly distributed throughout the complete building material or within the zones where damage is expected. In such way, healing will be more efficient. If the healing mechanism would not be dispersed as uniform as expected, part of a construction element may not show healing. This is unwanted, as a robust and uniform healing is needed, especially in terms of safe design of self-healing construction materials.

4.1. Visual Observation, Radiography, and Tomography to Study the Distribution

A first technique to study the distribution of the healing agent is by looking at the surface of cast elements or samples. By looking at a structure with the naked eye, conclusions can be drawn on the distribution. Furthermore, the distribution of microcapsules at a surface can be studied by means of microscopy,^[110–112,114] and the macropores formed by SAPs can be studied as well.^[87,144] The found capsules and macropores should evenly be distributed. Also, by looking at the formed SAP macropores, one can estimate the amount of swelling of the SAPs in terms of mixing water.^[122] This is interesting, as the correct amount of additional water needs to be added to the cementitious material. If too much water is added, the overall water-to-cement ratio is altered and increased.^[145] If too less water is added, the water-to-cement ratio is decreased, leading to a densification of the cementitious matrix^[87] and a higher amount of unhydrated particles needed to sustain autogenous healing.^[87,146] By microscopically monitoring the formed macropores and back-calculating-volumewise the absorption capacity, one can verify this.

X-ray radiography has been used by Van Tittelboom et al.^[147] to study the distribution of tubular capsules inside a concrete matrix. As damage is mainly expected near the bottom of concrete beams loaded in bending, a uniform distribution of capsules within this zone would be beneficial. While in some test series, long glass tubes or short glass capsules were connected to the lower reinforcement bars, in other series, glass capsules surrounded by a mortar layer were placed at the bottom of the mold and tended to flow toward the required zone during sample vibration. In the last series, glass capsules embedded in

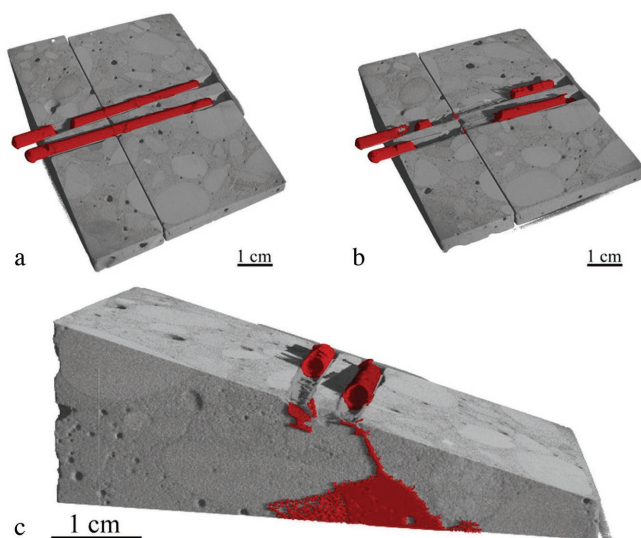


Figure 1. 3D illustration of the healing agent (red) in the different steps of the experiment: a) in the beginning of the experiment, when the glass tubes are still intact; b) after the movement of the smallest concrete prism has broken the glass capsules, thereby releasing part of the healing agent; c) a side view of the leakage of healing agent within the artificial crack. Reproduced with permission.^[141,142] Copyright 2018, Elsevier.

cement paste bars were added to the concrete during mixing. As capsules did not seem to survive the mixing process, even when protected with cement paste bars, they were further mixed in by hand. The molds of this test series were filled in two layers, which the lower layer containing the mixed in capsules. From the X-ray radiographic images it could be seen that when capsules were placed at the bottom of the mold, they indeed ended up in the required zone near the bottom of the beam. When capsules were mixed in by hand, a more or less homogenous distribution of the capsules through the complete concrete matrix was noticed, although the capsules were only added to the lower layer close to the bottom of the beam.

X-ray CT is an ideal technique to visualize the distribution of microcapsules within the cementitious matrix. A uniform dispersion is important to make sure that randomly existing cracks cross enough capsules to allow healing. A uniform distribution, without agglomeration, of polymeric microcapsules in a cementitious matrix was found by Lv et al.^[103,105] However, in order to have a good contrast and a clear visualization of the microcapsules, not only the capsule dimension is important to visualize them using X-ray CT, but also their X-ray attenuation has to be different from the matrix they are in. Using the XCOM web database of NIST the theoretical total attenuation coefficient of each component, such as microcapsules versus matrix, can be plotted for different X-ray energies. If no or low contrast is present, often doping agents, consisting of a higher atomic number and therefore a higher X-ray attenuation are added to either the capsules or the matrix.^[141] **Figure 2** shows the volume rendering and overall uniform distribution of microcapsules in a cement paste matrix.

X-ray CT has also been used to study the dispersion of microcapsules inside asphalt binders. As the shell of the melamine formaldehyde microcapsules used by Su et al.^[104] contains inorganic nano-CaCO₃ particles, the shape of the capsules could be easily identified on the CT images due to the density difference between the capsule shell and the bituminous matrix. The authors concluded that the microcapsules were homogeneously dispersed in the bituminous matrix without signs of capsule agglomeration. In the study of García et al.^[148] nano-CT scanning was used to study the distribution of steel wool fibers inside self-healing asphalt. Although fibers were noted all around the sample, which is important to reach uniform heating through induction, when comparing images showing all fibers with images showing only connected fibers, it was shown that not all fibers were connected and moreover that fibers tended to cluster.

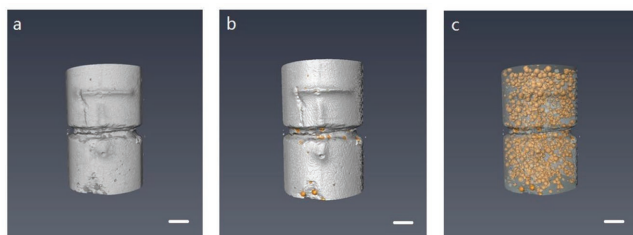


Figure 2. X-ray CT visualization process of microcapsules' embedded in a cement paste cylinder including a) volume construction, b) surface generation, and c) transparent adjusting. The scale bar is 2 mm for all three images. Reproduced with permission.^[105] Copyright 2016, Materials (Basel).

5. Techniques to Study the Trigger Mechanism

While some self-healing mechanisms require a mechanical trigger such as crack formation, others require a chemical, physical or thermal trigger. In this section, how nondestructive and minimal invasive testing techniques can be used to study these trigger mechanisms is described.

5.1. Notification of Healing Agent Leakage

After crack formation, release of the healing agent from the capsules can be noticed through visual observation of the sample surfaces.^[149,150] Successful release of the encapsulated healing agent mostly results in some healing agent leaching out of the crack.^[143] If healing agents with a very low viscosity, such as encapsulated minerals,^[150] water repellent agents,^[151] etc., are used they penetrate fast into the matrix. In the latter case, only a discoloration of the cementitious matrix will be noticed, but this also proves a successful triggering of the mechanism. Possibly, a colorant may be added to the healing agent to improve the discoloration on the sample surface.^[152]

5.2. Visual Notification of Capsule Rupture

In the study of Liu et al.^[153] X-ray CT was used to show that the creation of cracks (with a width varying from 20 to 50 μm) in a cementitious matrix triggered rupture of ethyl cellulose capsules containing a bacterial healing agent. Also Lv et al.^[105] used CT combined with data reconstruction and image segmentation software to investigate the crack zone in cementitious materials with self-healing properties and find a relationship between the size of microcapsules and their trigger behavior. Therefore, a small region around the crack was selected as region of interest and different materials were color labeled. The phenol formaldehyde microcapsules, the crack and the cementitious matrix were defined with a yellow, blue and gray color, respectively. To study the trigger behavior of the microcapsules, the upper half of the crack zone was isolated from the region of interest. As can be seen in **Figure 3**, part of the

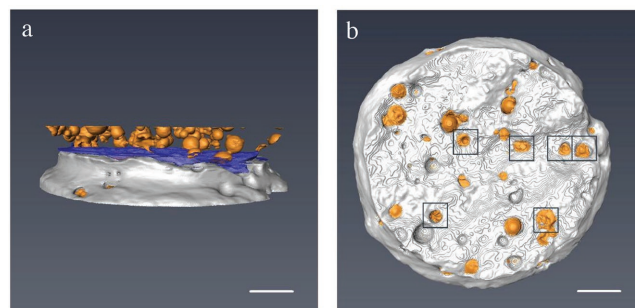


Figure 3. 3D reconstructed images showing the crack (blue), microcapsules (yellow), and cementitious matrix (gray): a) a selected section of fractured cement paste in the vicinity of the crack; b) a top-down view of crack surface. Ruptured microcapsules are indicated by a black square box. The scale bar represents 1 mm in both images. Reproduced with permission.^[105] Copyright 2016, Materials (Basel).

microcapsules was mechanically triggered by the crack, but also a large amount was not triggered of which some of them left behind voids as they were pulled out of the matrix. Performing this type of analysis for samples with microcapsules of different size ranges showed that for larger capsules (400–600 μm) 8.4% was triggered through crack formation, for medium size capsules (200–400 μm) 20.7% was triggered and for small capsules (50–200 μm) 34.7% was triggered upon crack formation. It could thus be concluded that smaller sized phenol formaldehyde microcapsules tend to be more easily ruptured through crack formation and have a lower change of being pulled out of the cementitious matrix.

5.3. Audible Notification of Capsule Rupture

In case mechanically triggered microcapsules are used to sequester the healing agent, successful triggering of the healing mechanism may be noticed as an audible pop sound at the moment of crack formation.^[150] These sounds are noticed after the maximum loading capacity of the element is exceeded and mostly correspond to small drops in the load–displacement diagram.

Previous studies have confirmed that AE analysis is a suitable method to investigate the activation of capsule rupture or fracture as well as crack initiation and crack propagation in concrete. It can be performed in two different ways, signal-based and parameter-based evaluation. A signal-based analysis may be used to postprocess each single recorded waveform. If for example, the signal to noise ratio of the AE acquisition is low, subsequent filtering or complex algorithms can significantly improve the evaluation.^[79,81,82,154,155] However, it must be recognized that this also leads to a distortion of the signal.

Depending on the evaluation method and the characteristics of sound wave propagation of the test object, good sensor coverage is necessary. By means of an additional localization of the detected acoustic emissions, the parameter-based AE evaluation of self-healing properties can be further verified. Tsangouri et al.^[156,157] showed that high-energy events can be localized and related to capsule fractures during crack initiation by a three-point bending test. Van Tittelboom et al.^[158] also combined the notification of audible pop sounds, with drops in load and AE analysis to proof capsule breakage and thus to proof triggering of the self-healing mechanism upon crack formation. In the latter study, cracks were created inside 50 mm \times 110 mm \times 500 mm concrete beams, containing encapsulated polyurethane, upon loading in a three-point bending test. By analyzing the energy of the AE events, capsule breakage could be clearly distinguished from crack formation. Moreover, not only during crack creation but also upon reloading high energy events were noted, proving that upon reloading additional capsules break and thus additional healing agent may be released. Events caused by capsule breakage were also localized and compared to the capsule position verified from the fracture plane as can be seen in **Figure 4**.

However, these investigations have also determined that detection of capsule fracture depends strongly on the accuracy of the localization. Since capsules are ruptured during crack formation, distinguishing these acoustic emissions from the

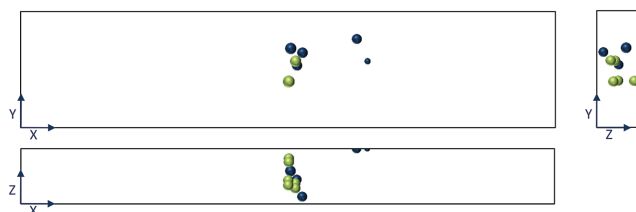


Figure 4. Location of tube fracture planes determined by means of AE analysis (blue dots) and measured from the cross section of the broken beam (green dots). Reproduced with permission.^[158] Copyright 2017, Elsevier.

high amplitude emissions released by concrete cracking is only possible when the position of the capsules is known or an energy-based analysis based on crack patterns is performed.^[147] If only a parameter-based analysis is conducted or reference test specimens are used to separate acoustic emission clusters, the complete waveform needs to be analyzed. In order to increase the reliability, surplus measurements with e.g., a large number of sensors are necessary.

Figure 5 demonstrates the detection of the crack formation during a three-point bending test in situ. A video can be found in the Supporting Information. The size of the acoustic emissions is correlated to the energy and is shown in red for the crack detection. Occurring high-energy acoustic emissions are separated and referred to capsule breakage, which are depicted in green. A verification similar to Van Tittelboom et al.^[158] confirmed these results.

When increasing the dimensions of the test specimens and introducing multiple crack formations from four-point bending tests, acoustic emission signals can increasingly be drowned in noise or characteristics of the often-used acoustic emission parameters (energy, frequency) are even more changed than for, e.g., lab-scale beams.^[159] Thus, if the distance between the acoustic source and the sensor placement increases, the signal becomes significantly weaker due to geometric spreading.^[160] Additionally, localization becomes progressively more complex

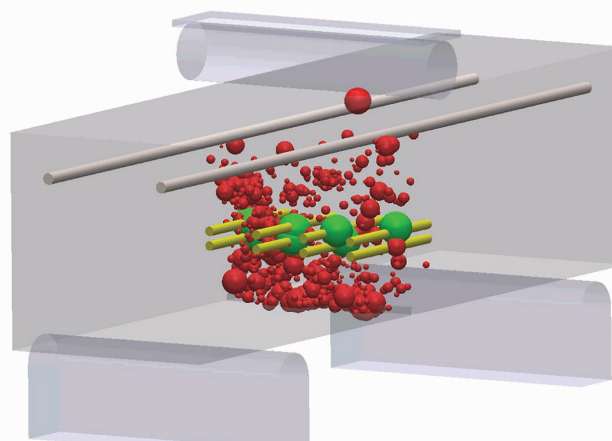


Figure 5. Detection of crack formation (red acoustic emissions) and capsule breakage emissions (green) during a three-point bending test with the specimen in gray, the reinforcement bars cylindrically in gray and the capsules containing the healing products in yellow.

due to the increasing migration of microcracks. Therefore, as specimen dimensions increase, the use of this nondestructive test method becomes more limited to detect capsule breakage and crack formation.

However, activation of the self-healing approach based on encapsulated polyurethane was confirmed by means of acoustic emission analysis for large concrete beams with dimensions of 150 mm × 250 mm × 3000 mm.^[143] Based on an energy analysis, a discrimination could be made between hits obtained due to crack formation during a four-point bending test and capsule breakage. Only in the case of capsule breakage, the energy received by all the eight transducers placed at the surface of the beam exhibited specific values showing the event.

6. Healing Efficiency

When the healing agent has reacted or the healing products are formed, the healing efficiency should be investigated. This can be done for cementitious materials, for asphalt, for masonry mortars and for other construction materials.^[161]

6.1. Visualization of Crack Closure upon Healing and Determination of Healing Rate

The crack closure can be evaluated by means of microscopic analysis. Either photography or light microscopy can be used. This technique can be applied for all healing mechanisms and different magnifications can be used. Microscopic analysis can be used to study one crack or multiple cracks. Not only wide cracks, but also narrow cracks can be investigated in great detail.^[162] Furthermore, by means of image analysis, the extent of healing, i.e., the visual closure of cracks, can be quantified.

If the healing efficiency is evaluated through a microscopic analysis of the crack, different evaluation strategies are possible. One way is showing the residual crack width as a function of the initial crack width. Thus starting from a bisector for no healing and with the curve shifting downward for healing as the crack width decreases.^[163,164] Another way is to investigate the percentage of closure as a function of the initial crack width. The higher the curve, the more healing occurred.^[22,86,122,165] A third way is to study the total crack and to determine pixelwise the amount/percentage of closure by comparing the total surface of a crack before and after healing.^[110,166] In the study of Roig-Flores et al.^[167] different crack geometrical parameters were measured and compared with water flow measurements before and after crack healing. The following crack geometrical parameters were considered: the maximum crack width along the whole crack length, the average crack width determined as the average of the width measured at five fixed positions, the estimated crack area which is calculated by multiplying the before mentioned five crack widths with their associated lengths and the crack area determined using graphic software which counts the black pixels, representing the crack, in the image. Best correlations were obtained from the relation between the water flow measurements and the estimated crack area or the average crack width. The correlation between the obtained water flow values and the maximum crack width or the crack area based on pixel

counting resulted in the worst relationship. Although, Roig-Flores et al.^[167] found a good relationship between the water flow test and some of the crack geometrical parameters, it should be noted that microscopic analysis only gives you an idea about the crack healing efficiency at the crack mouth while water flow tests may represent the healing efficiency of the complete crack. Based on the internal crack geometry, evaluation of the healing efficiency by measuring the width at the crack mouth will result in an overestimation or an underestimation.^[167] If the crack tip is having a lower width than the crack mouth, precipitates will mostly be formed at the tip.^[111] Also if the crack has a concave shape internal crack healing will be promoted but for cracks with a convex shape precipitates will most easily be formed at the crack mouth. Also Kanellopoulos et al.^[150] compared the healing efficiency obtained via crack area measurements with capillary water absorption tests. The absorption test only lasted for 4 h but allowed them to conclude that when glass encapsulated minerals are embedded in the matrix, healing materials are not only formed at the crack mouth but also deeper in the crack forming a barrier decreasing the capillary absorption.

Visually studying self-healing is interesting as a relationship between healing of mechanical performance and crack sealing can be found.^[122,166] This shows that a simple microscopic analysis of the formed healing products in a crack may already show that the material could regain part of its mechanical properties and durability. The amount of crack filling by healing products is monitored over time and can be repeated after a certain amount of time or healing cycles. A study after 3, 7, 14, and 28 d of healing is common when studying autogenous healing in cementitious materials.^[86,121,122] In this way, conclusions may be made in terms of the healing rate.

When bacteria are used to heal cracks in cementitious materials, the crystal growth and crack width reduction can be monitored in time by using microscopic analysis.^[93,127,153,168–176] Also when crystalline admixtures,^[115,136,163,167,177] expansive agents,^[163] autogenous healing,^[8,21,22,118–120,122,128–130,166,178–186] promoted and stimulated autogenous healing with SAPs,^[22,86,89–92,122] microcapsules with bacteria and other healing agents,^[93,110–112,187] the combination of bacteria and SAPs,^[188,189] and sodium-silicate saturated lightweight aggregates^[190] are studied, microscopic analysis can be used.

When samples are immersed during the healing process, drying of the sample surface may be required before a microscopic analysis of the crack can be performed. To do so, surfaces may be wiped dry, samples may be taken out of the solution some time before the analysis to dry or samples can be dried by compressed air.^[167] While not all researchers mention how they treat the samples before microscopic investigation, this might influence the measured healing efficiency. Drying of the samples may expose them to additional CO₂ in the air and this may enhance autogenous healing through calcium carbonate precipitation (because the process includes wetting and drying rather than continuous immersion). Exposure to CO₂ may also lead to carbonation of the specimens, resulting in a change in porosity near the surface. Drying with compressed air may loosen formed crystals in the crack, blowing them away and decreasing the measured healing efficiency. On the other hand, remaining fluids in a crack may cause erroneous results as the crack surface boundaries are not clearly distinguishable.

Microscopic analysis can be combined with fluorescence microscopy.^[143,191,192] However, epoxy needs to be inserted in the crack and this can be considered to be destructive. But in this way, the healing products can easily be investigated, using a portable UV lamp. If the crack depth morphology and/or the volume of healing crystals need to be known, a 3D microscope can be used.^[45,128,193] By using this 3D representation, conclusions may be drawn on the extent of healing, the morphology of the crystals and their structure. In this way, a 3D representation of the healed crack, the formed products or the healing agent is made. Images may also be taken from a distance with an SLR camera, which can also be employed on site to study the fracture and healing behavior.^[194] Image analysis afterward may determine the crack closure. This so-called digital image correlation (DIC) is a technique to study relative movements such as crack formation. A speckled pattern is drawn on a specimen and the dots serve as coordinate system in which strains can be determined. The pictures are recorded as a movie or different pictures can be taken with regular time intervals, even without the use of a speckle pattern to register the formation of cracks in large specimens.^[195] In the study of Isaacs et al.^[196] DIC was used to study crack closure of mortar beams posttensioned with shrinkable polymer tendons. In the study of Tsangouri et al.^[197] DIC was applied on self-healing concrete with encapsulated polyurethane to deduce the healing efficiency from the visualization of the damage recovered zone upon reloading of the beams. When tests are performed on a large scale and multiple cracks are created DIC could be a very interesting technique to monitor the opening of all crack mouths.^[143] In this way the healing efficiency of every crack can be related to the initial crack width.

6.2. Chemical and Physical Composition of Formed Healing Products

In order to provide a deeper insight into the nature of the healing phenomena, the morphology, the crystal phases and the chemical composition of the investigated healing products, SEM and EDX can be used. It is possible to perform line scanning or surface scanning of the sample. In this way, the healing products can be studied in time and as a function of the location. Bacterial precipitation can be studied qualitatively and quantitatively using the SEM technique.^[126,127,169,171,172,174,175,198–201] Based on counting of bacteria, conclusions may be drawn on their viability and ability to precipitate. The composition and the elemental analysis can state something about the usefulness of the different types of bacteria studied. Studying the precipitated healing products with SEM/EDX was applied for crystalline admixtures and geomaterials,^[115,116,136,177] for autogenous healing,^[21–23,121,202–205] healing of lime mortars,^[206] healing through embedded microcapsules,^[100,110,111] healing by porous silica or lightweight aggregates as a capsule or carrier for chemical or biological healing agents,^[138,194,207] SAPs^[22,91,122,123] and expansive powder minerals,^[187] among others. All these healing techniques result in different products, being formed and/or precipitated. By using SEM/EDX, quantitative conclusions may be drawn on the overall chemical composition and structure of the formed healing products. In this way, differences in precipitated healing products and where they are formed can be investigated in detail. An example is shown in **Figure 6**. Fukuda et al.^[208] studied the healing efficiency in the interior of the crack of ultrahigh performance concrete when

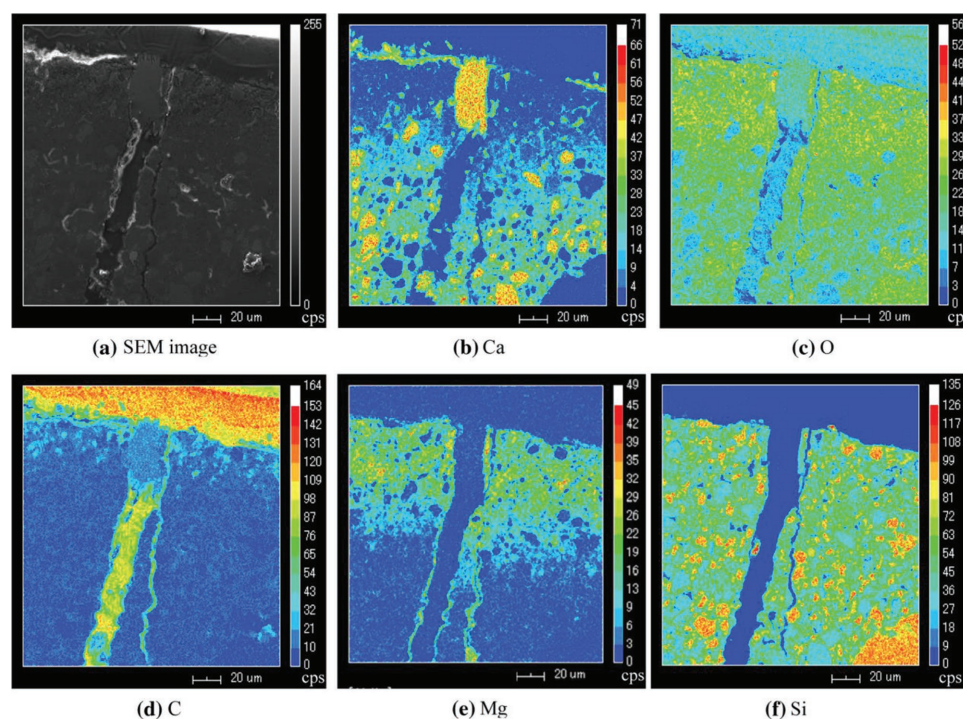


Figure 6. Results of SEM/EDX analysis of healing products formed in ultrahigh-performance concrete when being exposed to seawater. a) SEM image, b) Ca mapping, c) O mapping, d) C mapping, e) Mg mapping, and f) Si mapping. Note that cps indicates count per second. Reproduced with permission.^[208] Copyright 2014, Springer Nature.

being exposed to seawater by SEM/EDX analysis. SEM/EDX was performed on a surface sawn orthogonal to the crack to determine the composition of the sealing deposits, as shown in Figure 6. From the SEM images it was noticed that precipitates mainly formed close to the crack mouth and on the sample surface. A few more μm scale precipitates were also noticed inside the crack. Elemental mapping by EDX of Ca, Mg, C, Si, and O learned that the sealed crack region mainly consisted of Ca, C, and O, which led to the conclusion that sealing was obtained through CaCO_3 precipitation. On the sample surface a layer of brucite was noticed which was expected due to the exposure to seawater.

Electron probe microanalysis (EPMA) can be used for the elemental analysis of the formed healing products in steel-fiber reinforced cementitious materials.^[193] It is a technique similar to the SEM-EDX analysis and uses a beam of electrons, which are fired at a sample. The X-rays, which are emitted, are detected by an electron microprobe that can tell us something about the composition of the studied material. The big difference with SEM is the scale as characteristics on the micrometer scale can be investigated. EPMA can be used to study the healing products and salts in terms of the observed X-ray spectra.^[193] Another analogous technique to SEM-EDX and EPMA is Raman spectroscopy. When comparing the obtained spectra for different crystals, the composition of a studied material can be determined, especially when comparing profiles from uncracked and cracked areas.^[121] Raman spectroscopy uses a laser light to react with molecular vibrations, shifting the energy of the laser photons. This gives information about the constitutional elements of the material studied, i.e., the formed healing crystals. If a small powder sample can be extracted, X-ray diffraction and/or Fourier transform infrared spectroscopy (FTIR) is also an option to study the formed healing products in autogenous healing and bacterial healing.^[90,91,171,172,190,202,203,205] as well as attenuated total reflectance (ATR) FTIR.^[100,138,187] XRD measures the angles and intensities of diffracted incident X-ray beams to determine the molecular structure of a crystal. The qualitative analysis of the obtained phases can be done by means of Rietveld refinement.^[126,137,138] FTIR studies the absorbed or emitted light in a material in a wide spectral range to determine the composition of the material. ATR-FTIR studies the reflectance in a micrometer range.

TGA can also be used to characterize the obtained healing products.^[86,91,137,138,175,179,194,199,205,209] TGA can also be combined with differential scanning calorimetry (DSC).^[207] DSC is a thermo-analytical technique to study the amount of heat required to increase the temperature of a sample compared to a reference. It can be used to measure properties such as fusion and crystallization events and the glass transition temperature of materials, oxidation and other chemical reactions. The phase diagrams can be used to study the formed products upon healing.^[207] DSC is mostly preceded by TGA as TGA can determine whether or not a material degrades at certain temperatures. If this is the case and the material is degrading, the DSC would give erroneous results. One needs to mention that a certain small amount of material is needed to conduct both tests. As the material is destroyed, one may also classify these tests as being destructive. However, in most cases, the amount needed is limited that it can be accepted as being minimal invasive testing.

6.3. Visual and Thermal Analysis to Assess the Healing Performance

Self-sealing can be investigated by the naked eye. A nice example is the use of a glass sheet at one side of a cracked specimen, providing a direct view on the crack face through the glass.^[210] In the latter research, the mortar with embedded water-swelling rubber particles showed a clear sealing behavior. Furthermore, X-ray CT was used to visualize the self-sealing efficiency and a decrease in water permeability was seen due to the physical blockage by the swelling rubber particles.^[210] Neutron radiography can also be applied to study the regain in impermeability of a mortar containing SAPs upon water intrusion.^[124] By imposing a water head and monitoring the water through a crack, the sealing can be investigated.

For self-healing mechanisms with embedded heating devices, the 3D thermal distribution can be interesting. By analyzing the thermal distribution around a crack, the healing efficiency can be studied.^[211] As the self-healing mechanism had an arrangement of heating devices and thermal plastic pipes containing the repair agent, the heating serves as an assessment for the healing capacity. Next to the visual appearance of the healing agent, the selective melting of the organic film pipe and the release of the repair agent into the crack was monitored and seen as a temperature increase. As the healing progressed, the temperature decreased, showing the healing efficiency.^[211]

To compare the healing efficiency of asphalt with steel fibers (healing through heating of fibers) at the one hand and steel slag aggregates (healing through heating of aggregates) at the other hand, Sun et al.^[212] made use of infrared thermal imaging. As in these asphalt mixtures, healing is triggered by heating, it is important that exposure of the material to induction of microwave heating results in a uniform temperature increase of the material. Infrared thermal analysis was used to study the temperature increase, the temperature distribution and the heating rate. They concluded that a more uniform temperature distribution was obtained when self-healing asphalt with steel slag was used as the aggregates occupied the main volume while the fibers only occupied a small volume. Also Menozzi et al.^[213] made use of thermographic imaging to study the behavior of self-healing asphalt with steel particles during induction heating.

6.4. Distribution and Amount of Healing in the Interior of Building Materials

Most nondestructive techniques provide information from surface properties. No information about the interior structure or the ongoing processes can be obtained. In concrete, some healing techniques stimulate crystal formation near the surface. Sometimes, almost no healing is found in the interior of the sample. By only studying the surface, false conclusions may be drawn. Therefore, it is interesting to use high-tech techniques to study the formed healing products in the interior of a sample. Preferably, this should be done nondestructively and in great detail with sufficient resolution. Self-healing can be studied in the interior of the sample by using neutron or X-ray computed radiography or tomography. Voids, reinforcement,

aggregates and the cementitious matrix can be distinguished based on their difference in density. Both techniques are used to visualize the interior of a sample, as well as the formed healing products, crack openings and healing product distribution.^[124,149,151,179,214,215] The technique may also be used to quantify the amount of healing (volume of healing products and distribution along the crack) next to qualitatively studying the healing products.^[123] In this way, solid conclusions may be drawn on the amount of autogenous healing capacity in the interior of specimens,^[123,204] the amount of bacterial calcium carbonate crystallization or precipitation by a bacterial treatment^[189,216–218] or the amount of polymerization of polyurethanes from tubular capsules.^[149,151] The healing can also be studied as a function of time by subsequent imposed healing cycles or water curing.^[179] In the research study of Olivier et al.^[179] the self-healing kinetics of cementitious materials containing ground granulated blast furnace slag was quantified through regular analysis by X-ray CT. It was shown that crack healing also occurred at the inside and this with two-stage kinetics: faster during the first weeks after cracking and then slowing down. A similar analysis was performed to study the self-healing efficiency of asphalt mixtures containing encapsulated rejuvenator^[219,220] or steel particles to induce healing through induction heating.^[213] In the study of García et al.,^[219] CT scan images of asphalt mixtures containing capsules were obtained for samples before and after cyclic loading and after healing. The porosity minus the initial air void content was taken as an indicator for crack healing. While one sample contained 4.1% air voids before cyclic loading, this amount increased to 8.3% after cyclic loading due to the initiation and propagation of cracks. However, after allowing the time for healing through release of oil from the capsules the air content decreased toward 6.4% due to crack healing. These results prove that about 45% of the cracking damage disappeared due to healing. Also Menozzi et al.^[213] compared the air voids before and after healing through induction heating to investigate the recovery of fatigue damage. In addition, they analyzed the variation in the number of air voids along the sample depth. As a homogenous distribution was noticed, it was concluded that a distributed temperature profile along the height of the sample caused by induction heating of the asphalt matrix had no influence on the healing efficiency. Although the temperature was higher at the top of the specimen, a homogenous distribution in number of air voids was found.

When the X-ray radiography images are combined after scanning the sample over 360° to obtain a tomography,^[45,123] this approach can be used to confirm the creation of localized bridges (healing product) between the cracks faces and can confirm their location within the crack.^[45] The results found by the latter researchers corresponded with other nondestructive tests used in that research, which were nonlinear modulation of ultrasonic coda waves and 3D microscopy. Precipitation upon healing of construction materials in seawater or in fly-ash systems can be studied as well.^[221–223] In the latter studies, crystal precipitation is clearly seen after performing repeated X-ray radiography scanning before and after healing. The healing conditions (healing in seawater) and the mixture composition (specimens containing fly ash) had no influence on the efficiency of the X-ray radiography techniques as the samples were

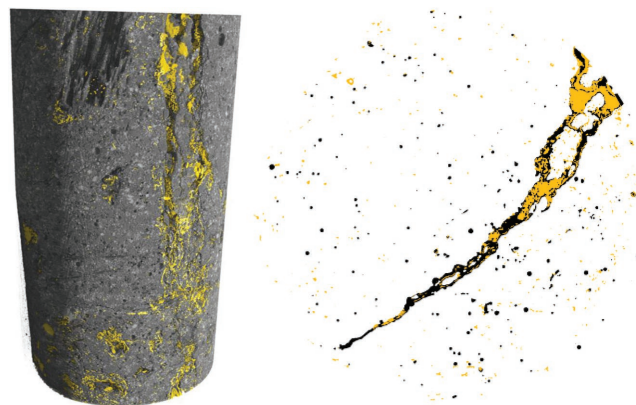


Figure 7. X-ray microcomputed tomography of the precipitation in an autogenously healed cementitious specimen containing superabsorbent polymers. Reproduced with permission.^[122,123] Copyright 2015, Elsevier.

dried before scanning and the precipitation could clearly be distinguished.

An example of the amount of autogenous healing promoted by SAPs studied by means of X-ray CT can be found in **Figure 7**.^[122,123] A scan was made prior to healing and after healing. By subsequent image analysis and subtraction of both data sets, the amount of precipitation could be monitored and quantified. In the right-hand side, a slide perpendicular to the specimen's axis is shown. The X-ray CT technique can therefore easily be used to study the precipitation in the interior of the crack. Furthermore, it is possible to study the porosity and the pore size distribution. X-ray CT was also used by Fukuda et al.^[208] to visualize the progress of crack sealing in cementitious materials by extracting the precipitated region. It was confirmed that healing occurred mainly near the outermost part of the sample. In the mostly sealed region (0–0.3 mm from sample surface), 70% sealing was obtained after 49 d exposure to seawater. Moreover, it was concluded that the maximum sealing rate was obtained in the timeframe of 7–21 d immersion and this rate amounted to 3.7%. Heating and recurring in water may also be studied by means of X-ray CT.^[224] This is important in terms of concrete damaged by fire. The percolated crack space could be quantitatively observed and the reduction in crack volume was studied in 3D and as a function of time, showing healing under water supply.^[224] Studying the connected pore space and the pore size distribution was another way of proving the efficiency of the curing in time.^[224]

In steel-fiber reinforced cementitious materials X-ray CT can be used to visualize the debonding of the fiber.^[193] This information is needed to study the fracture mechanics for multiple cracking, which is an interesting property as it leads to small cracks which can be healed by means of autogenous healing.^[193] This debonding can be seen by taking X-ray micrographs prior and after testing.

lv et al.^[225] used X-ray CT scanning to confirm visually the results obtained with the binder bond strength (BBS) test with regard to the self-healing behavior of bitumen and its influencing factors. Therefore, X-ray CT scan analyses were performed at set time intervals during the healing process. Air bubbles and cracks in the samples decreased over time and different stages were distinguished during the healing process:

moving of adjacent air bubbles toward each other and merging into one bubble (gathering), air bubbles at the edge of the film are moving outside (moving) and air bubbles taking a round shape during healing (rounding). The CT analysis allowed to investigate the influence of different parameters such as the healing temperature and time, the effect of a polymer modifier and the effect of wet or dry healing conditions.

García^[226] studied the crack healing efficiency in asphalt by CT. He wanted to prove that the speed of healing of thermally induced self-healing asphalt (with steel wool or steel fibers) increases with increased temperature according to the Arrhenius equation. Therefore, broken samples were healed at different temperatures and CT was applied over time at elevated temperature to visualize the healing efficiency. The time required for complete healing was used to calculate the activation energy. In **Figure 8**, the subsequent X-ray CT images obtained for a sample heated at 70 °C, are shown. Zones where the crack faces come together again, or where the crack is healed, are represented in white. It can be noticed that healed sections grow from the contact points and that healing is more intense in the bottom part of the specimen.

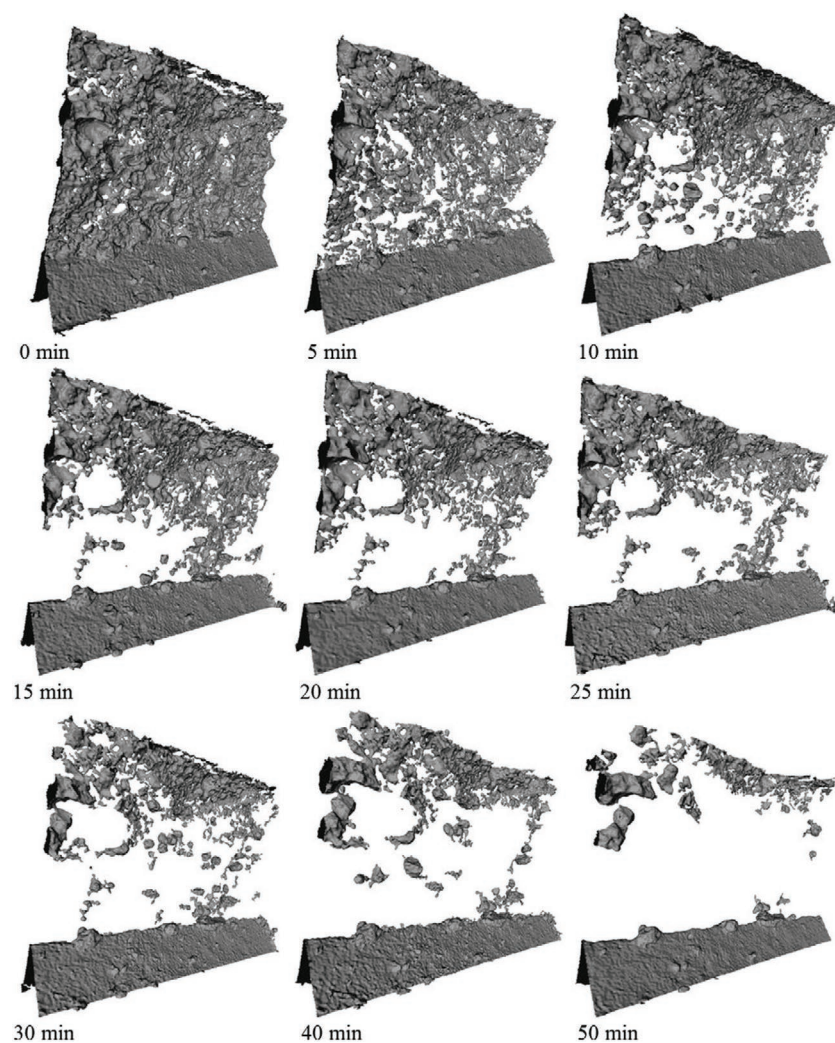


Figure 8. CT reconstructions of a crack in asphalt healed at 70 °C showing healing in time (white color). Reproduced with permission.^[226] Copyright 2012, Elsevier.

6.5. Water (Im-)Permeability to Verify the Effectiveness of Healing and Closure of Cracks

The main reason to implement self-healing properties in concrete materials is to improve the durability of concrete structures through an increase of the tightness after cracking. Therefore, an ideal technique to measure the healing efficiency is by measuring the water permeability after crack repair. A low-pressure water permeability test may be used for smaller specimens.^[86,214,227–229] These tests use cylindrical specimens, which are cracked. Starting from an imposed water head and the timing of a certain water flow, the water permeability coefficient could be calculated. However, as a cracked cylindrical specimen is needed, these tests are often considered to be of destructive nature. However, analogous tests may be applied on concrete elements without the need to drill cores.^[143] One way is to position a water permeability test setup directly on the specimen under investigation such as a concrete beam. Van Tittelboom et al.^[143] studied the self-healing efficiency of SAP and encapsulated polyurethane on large-scale concrete beams by gluing water basins over separated cracks to investigate the possible physical sealing of a crack. While it was the idea that the decrease in water column, of the pipette placed on top of the basin, would give a correct indication of the sealing efficiency, it was noted that values did not correspond with the microscopic investigation of the crack sealing efficiency. It was not possible to prove the sealing from this experiment as neighboring cracks were interconnected and water started to leach from these cracks. However, when the sealing efficiency of separated cracks in large-scale elements needs to be investigated, the authors believe that this can be a valuable technique. Another test is a water leakage test which can show the recovery of water-tightness of a cracked mortar plate using a self-healing system.^[211] It is a testing method to measure the water permeability through coating materials as described in the Standard JIS A 6909. A pipette funnel and the testing plate were sealed with a silicone gel material. The test was carried out until penetration of a water volume of 5 mL through the surface was reached. The time needed served as an assessment of the quality of healing. This simple test could already show whether or not a crack is completely sealed. Precautions should be made for the good adhesion of the test setup to the overall material, as leaks should be avoided.

A sample can also be submerged or partially submerged to study the healing efficiency.^[230] However, you may alter the hydration degree and a sample cannot be submerged entirely in practice. A capillary absorption test may show the regain in liquid tightness when using various self-healing

mechanisms.^[114,231] In these tests, the amount of water absorbed is gravimetrically compared for the different systems. This can also be combined with neutron radiography measurements.^[124,151,214,215] In these tests, neutrons are passed through a specimen when it is absorbing water. As neutrons are easily scattered by a hydrogen atom, differences in gray levels can be seen. In this way, the water movement, capillary rise and the water-front can easily be studied. Furthermore, by using a quantitative analysis technique, the amount of water absorbed can be calculated and compared to the gravimetric results.^[232] In this way, the water movement at distinct locations can be studied, together with vertical and horizontal water movement. The technique showed good healing for cementitious materials containing encapsulated healing agent^[151,214,215] and a sealing effect for cementitious materials containing SAPs as water movement was prevented due to their swelling capability.^[124]

6.6. Use of Acoustic Techniques to Verify Healing

The most commonly used ultrasound evaluation methods for the detection of self-healing effects in cementitious materials are ultrasonic pulse velocity (UPV), surface transmission, diffuse ultrasound and coda wave interferometry (CWI). A well overview with suitable studies is found in Ahn et al.^[68] It remains to be stated that the different modifications of ultrasonic measurement techniques are suitable evaluation methods for monitoring structural damage as well as the performance of self-healing of cementitious materials. However, since there is no standardized test procedure for the characterization of damage and its repair, data acquisition and analysis are conducted on an individual basis. In order to be optimally capable of verifying the results, a detailed description of the test procedure is necessary.

The self-healing efficiency of concrete using different types of healing agents may be evaluated through artificially formed and controlled microcracks. In ultrasonic testing, propagating elastic waves are mainly reflected and scattered at the interfaces between the crack walls. This presupposes that the crack location is known and lies between the sensors, otherwise no variation in

the signal would be recognizable. With increasing crack growth, the behavior of the transmitted signal also changes. Depending on the selected measurement setup and sensor placement, analysis of the corresponding signal analysis can thus provide conclusions about the crack development. In addition to the test material properties, the type and application of the transducers is an important component for the detection of variations in the signal patterns. In this context, a reproducible measurement procedure is essential to obtain a quantified result on self-healing efficiency. To avoid decoupling effects by the transducer ultrasonic continuous monitoring enables a quantification of changes due to cracking, failure and healing.

Figure 9 presents analysis results of a continuous monitoring test from the HealCon project on a reinforced concrete test specimen (550 mm × 150 mm × 150 mm) and commercial surface-coupled shear wave transducers. In contrast to the UPV method, the correlation coefficient (between the ultrasonic waveform of the pretested specimen and the damaged specimen) was used to distinguish small changes in the material.^[233–235] The objective within the project was to investigate the crack formation phase (Figure 9, Phase 1), the relaxation behavior phase (Figure 9, Phase 2) due to the existing reinforcement as well as the crack sealing and healing phase (Figure 9, Phase 3) due to manually injected polymers. The cracks were induced by a crack-width controlled three-point flexure test.^[236] After failure, the correlation coefficient drops to slightly below 0. Due to the elastic extension behavior of the reinforcement, a slight crack closure after stress relief is triggered, which is reflected by a rapid increase in the correlation coefficient. The relaxation phase remained stable for nearly 50 h. While the crack is sealed and the polymers form a force-fit bond between the walls of the cracks, ultrasonic signals show a partial recovery to the initial condition. This example demonstrates that the continuous ultrasonic technique can be used for condition monitoring of cementitious materials during damage and subsequent restoration. However, it is important to note that the cementitious material with healed cracks constitutes a new type of material compound, which was not considered when calculating the correlation coefficient for the filling and hardening phase (Figure 9, Phase 3). A conclusion on the quality of crack healing (polymer distribution, rebond characteristics,

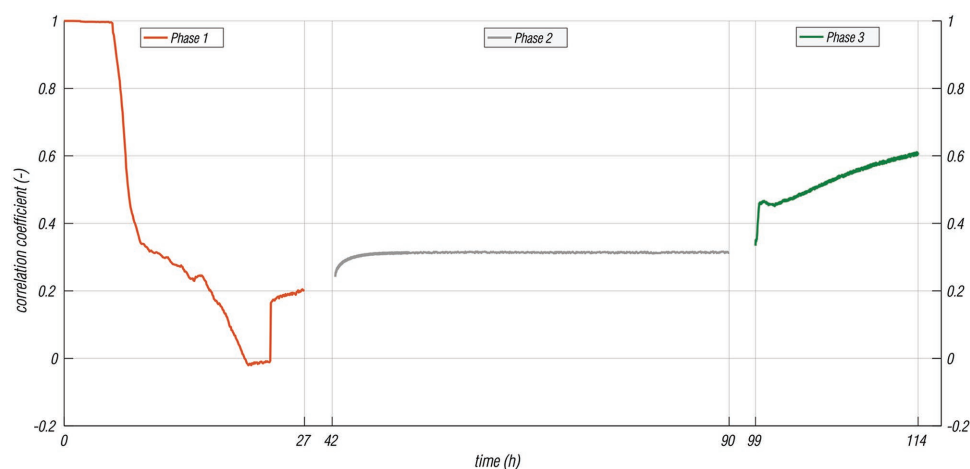


Figure 9. Analysis of a continuous monitoring test with surface-coupled shear wave transducers showing the crack formation phase, the relaxation behavior phase, and the crack sealing and healing phase.

etc.) cannot be made without additional examination methods (reloading curves, numerical analysis).

Granger was able to demonstrate in a modified and system-optimized experiment autonomous crack healing effects on ultrahigh-strength concrete during water-immersion tests by using the time reversal technique.^[237] However, the transducer remained coupled in this investigation as well. The Coda wave interferometry is regarded as one of the most promising test methods for examining acoustic transit time variations in the ultrasonic signal. By mixing nonlinear coda waves with low-frequency swept pump waves, small cracks can be detected globally. Based on studies by Zhang et al.,^[238] Hilloulin et al.^[46] optimized this evaluation method for detecting microcracks in cementitious materials. Finally, in combination with additional nondestructive techniques such as 3D microscopy and X-ray tomography, autogenous crack healing of mortar samples could be demonstrated.^[45] As mentioned before, it is possible to observe and differentiate crack failure, filling and hardening with a continuous sensor coupling. If an examination is to be performed at individual time intervals, e.g., after water permeability tests or in field and a reinstallation of the testing setup is required, inconsistencies within the data acquisition associated with transducer coupling conditions should be eliminated. Approaches with air-coupled transducers have already shown that reproducible and consistent results for the detection of material parameters and microcrack damage are possible even without direct sensor coupling.^[239–242] Especially for the application on large test specimens this method could have a great potential for monitoring self-healing. Due to the absence of coupling effort, measurements can be carried out much faster and more cost-efficiently.^[243]

Additionally, studies using piezoelectric transducers (smart aggregates or SMAGs) embedded into the concrete matrix have shown that the ultrasonic pulse velocity method is able to monitor the damage and healing development in situ.^[62,244] If the transducers are embedded during production of the test object, the piezoelectric sensor coupling can be substantially simplified. However, it is necessary to assure that no coupling changes between the transducer and cementitious matrix are caused through stress–strain effects. Based on this knowledge, further research was carried out to develop low-cost and application-oriented transducers.^[245]

To assess the autogenous healing efficiency of concrete, In et al.^[41] made use of in situ monitoring by diffuse ultrasound. With the progress of healing, the arrival time of maximum energy (ATME) decreased and the effective diffusivity increased until the initial values found in uncracked concrete.^[246] Moreover, it was noticed that the evolution in ultrasonic diffusivity exhibited a quite similar trend compared to the evolution in crack width. A larger fluctuation was noticed in the results of the ATME measurements. This was most probably caused by the fact that the measured ATME is influenced by local bridging between the two crack faces. Therefore, the authors concluded that diffusivity is a more reliable and robust indicator for crack healing in concrete than ATME.

If heating needs to be applied to induce healing, the healing process can be monitored using ultrasound. Franesqui et al.^[247] studied self-healing of surface cracks in bituminous mixtures after microwave heating was investigated. The ultrasound technique was useful for tracking the crack depth over time, the assessment of the crack depth evolution over time and the

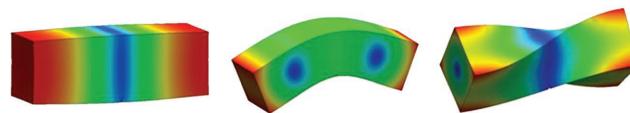


Figure 10. Schematic design of different types of resonance moduli: longitudinal (left), flexural (middle) and torsional mode (right).

effectiveness of the self-healing approach. The method allowed to determine the crack depth immediately and even for microcracks unobservable to the naked eye. After placing a specimen in an oven, a visual inspection was first carried out to verify the healing of the cracks. Afterward, subsequent monitoring was done. Ultrasonic testing showed that healing began at the crack tip and spread toward the surface.^[247]

Impact resonance analysis is applied to determine the elastic material properties of mortar and concrete test specimens. By evaluating the resonance frequencies, this nondestructive technique allows to give global information about the structural damage conditions by changes in the natural frequency of vibration. Based on solid media considered to be totally elastic, homogenous and isotropic, the dynamic modulus of elasticity (or Young's modulus) of a cementitious specimen is mainly related to its dimension, elastic material constants and density. Therefore, the elastic and also shear modulus of an object can be calculated from the measurement of the longitudinal, flexural (transverse) and torsional frequency of vibration and the corresponding mathematical relationship (refs. [69,70,248]—a feature that is well established in scientific research and material testing^[71–75]). This design of different types of resonance moduli can be found in **Figure 10**. As a conclusion, material changes due to physical and chemical stresses are detectable by the change of the natural frequencies of the entire system.

Due to controlled laboratory test conditions in this study, degradations are fully related to damage processes based on crack-width controlled three-point bending tests. Finally, self-healing efficiency is validated relatively by comparing the individual test specimens in each single state, i.e., initial, cracked and healed. Due to more stable results the first longitudinal, flexural and torsional eigenfrequencies are evaluated to calculate the Young's modulus and the shear modulus. Finally, these variations should be, in terms of magnitude, outside of the systematic and statistic error.

In order to be able to use the described ultrasonic evaluation methods for a qualitative validation of the healing efficiency, further research work is needed. It has been shown that the amount and distribution of, e.g., polymer-based precursors inside a crack for healed specimens depends on a large number of parameters and consequently can fluctuate significantly. In order to be able to determine the quality assessment of crack sealing not only globally, the resolution of the characteristic wave propagation has to be improved. A suitable method is a scanning or tomographic US measurement based on the UPV evaluation using surface-coupled transducers.^[249] First approaches to detect the partially crack closure due to autonomous healing with epoxy based precursors are presented in **Figure 11**. A reinforced concrete beam (550 × 150 × 150 mm, steel bar ϕ 6 mm) with artificially initiated crack formation in the middle section was tested by longitudinal wave transducers. Indirect transmission measurements were performed at an even distance of 2 cm along the cross-section width. The

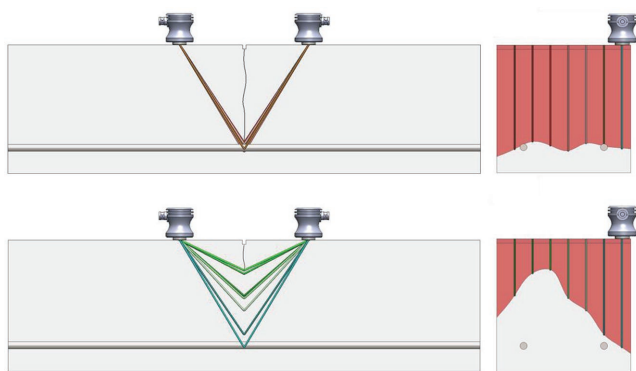


Figure 11. Crack depth calculation by determination of the transit time of the longitudinal wave in ultrasonic transmission mode (top). Measurements were conducted after the three-point bending test without load. Ultrasonic transmission measurement after hardening of the polymers (bottom).

crack depth was calculated by determining the transit time of the longitudinal wave propagation (top in Figure 11). If a contact bond of the crack flanks occurs while the healing process, the transit time is reduced (bottom Figure 11). The result after hardening of the healing agents is shown in Figure 12. It reveals that the crack depth corresponds to the dispersion of the epoxy.

7. Healing Performance

If the healing is successful, its performance over time needs to be studied. In this section, different nondestructive and minimal invasive techniques to study the healing performance of construction materials will be discussed.

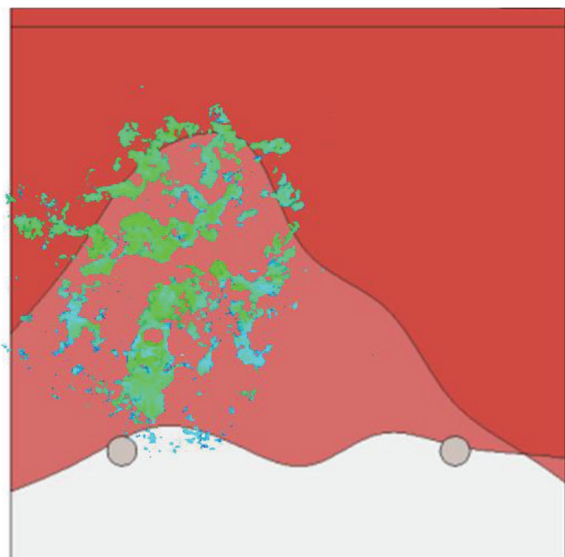


Figure 12. Schematic cross-section view of the crack zone of a concrete beam. Red areas mark the determination of the crack depth by UPV method (comparable to Figure 11). In parallel, additional fluorescent pigments (green) within the epoxy precursors mark the area of self-healing.

7.1. X-Ray Analysis to Study Corrosion Inhibition of Rebars and the Overall Healing Performance

Van Tittelboom et al.^[250] made use of X-ray radiography to study the performance of cracked mortar samples containing encapsulated polyurethane while being exposed to an accelerated corrosion test. For both, cracks orthogonal to and longitudinal with the direction of the reinforcement, it was noticed that when standardized cracks were autonomously healed through release of encapsulated polyurethane, the onset of reinforcement corrosion could be delayed. While for the reference samples pitting corrosion of the rebars was clearly noticed at the vicinity of the crack, the onset of corrosion could be delayed through self-healing. In addition to a qualitative evaluation also a quantitative analysis of the radiographs was performed and it was shown that the loss in reinforcement cross section was largely decreased due to embedment of encapsulated polyurethane.

Dong et al.^[101] used X-ray CT to study the performance of a chemically triggered self-healing system to inhibit corrosion of rebars in cementitious materials. Both, reinforced reference samples and samples with embedded ethyl cellulose microcapsules containing sodium monofluorophosphate or sodium nitrite were exposed to an accelerated corrosion test. X-ray CT image analysis was repeatedly applied after each test period to monitor the corrosion loss ratio of the embedded rebars over time (Figure 13). After dismantling of the samples, rebars were investigated by means of ESEM equipped with texture element analysis microscopy (TEAM) to verify the CT image analysis. It was shown that the identification of steel, corrosion products and mortar with penetrated corrosion products was consistent when using both techniques.

Another construction material for which the self-healing performance has been studied by high resolution synchrotron CT, is the annular cement and the cement plugs of wellbores.^[141,251–255] The use of depleted oil and gas reservoirs for capture and storage of CO₂ is considered as one of the promising solutions to reduce global emission of greenhouse gasses but first the potential problem of CO₂ leakage through the fractured cement needs to be addressed. While recent works have proven that cracks in cement tend to heal, and thus the permeability decreases, when being exposed to CO₂, this seems only valid at nonflow conditions. When the CO₂ is flooded through fractured samples, as will be the case for the cement in the wellbores used for CO₂ storage, it has been noticed that the permeability first increases (due to CaCO₃ dissolution and the formation of an amorphous silica layer) and then remains constant. In the study of Chavez Panduro et al.^[251] in situ X-ray CT was successfully applied under realistic subsurface conditions (elevated temperature, high pressure and presence of CO₂ saturated brine) onto a cured Portland cement sample with an artificially engineered leakage path. As can be seen in Figure 14 carbonation of the bulk cement, self-healing of the leakage path and leaching of CaCO₃ could be visualized and quantified. Moreover, the precipitation of CaCO₃, which is most important for healing of cracks in the fractured cement, was found to be favored in confined regions having limited access to CO₂. In contrast to the synchrotron CT experiments, currently similar experiments are also possible in lab environment using

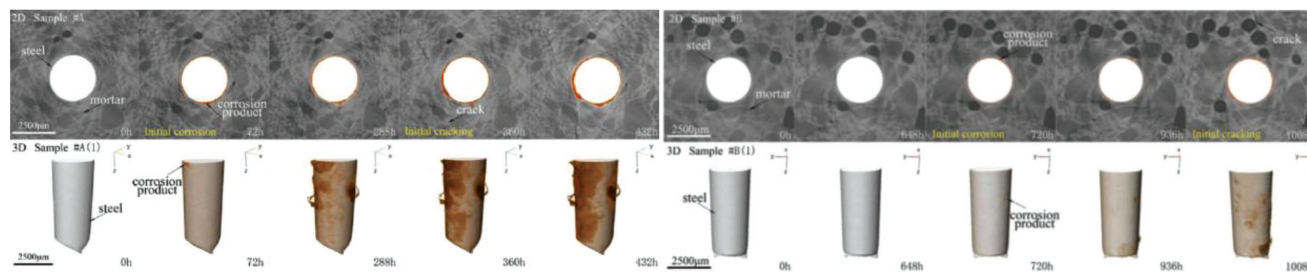


Figure 13. Reconstructed CT images visualizing the accelerated corrosion process. Left: Reference sample. Right: Sample with embedded EC capsules containing sodium nitrite. Upper: 2D image of the sample. Lower: 3D image of the rebar and the corrosion products. Reproduced with permission.^[101] Copyright 2018, Elsevier.

dedicated X-ray scanners where even reservoir conditions can be simulated in the framework of the study on CO₂ sequestration processes in fractured reservoir rocks.^[141]

7.2. DIC, Visual, and Acoustic Analysis to Monitor the Healing Performance

AE analysis has been used in parallel with DIC to study the healing performance in cementitious materials with two different types of encapsulated polyurethane, a rigid one and a flexible one.^[256] Samples containing an encapsulated polymer precursor were cracked, to trigger the healing mechanism. After curing of the healing agent, samples were reloaded while being equipped with an AE sensor. At the same time, the strains on one side face of the sample, were a black-white speckle pattern was foreseen, were monitored with a pair of DIC cameras. Based on hit counting, normalized energy and rise angle, a discrimination could be made between the healing performances of both polyurethanes. Detection of polyurethane failure through AE analysis was only possible in case of failure due to brittle fracture of the rigid polyurethane, which generated high energy acoustic events. DIC confirmed that there was a progressive widening of the crack healed with the flexible polyurethane (which could not be noticed by AE) while there was a sudden

widening of the crack healed with the rigid polyurethane (which could be noticed by AE), as shown in **Figure 15**.

In another study^[143] by the same research group, the performance of crack healing by embedded SAP was compared to the performance of crack healing by encapsulated polyurethane. Therefore, cores were drilled from the crack zones of the healed concrete element after reloading. These cores were injected with a fluorescent dye and microscopically investigated under fluorescent light. It was shown that only the polyurethane was able to follow the crack movement upon reloading as ingress of epoxy resin was prevented.

Depending on the type of polymers used, varying strengths of mechanical rebonding of the crack surfaces are obtained. Thus, similar to the AE analysis studies on the detection of capsule breakage, polymeric failure can generate acoustic emissions while reloading a repaired mortar or concrete beam. Other factors which affect the healing performance and at the same time the acoustic emission analysis, apart from the encapsulation technique, are the viscosity of the precursors or the stiffness after curing.^[158,231] Depending on the propagation of the polymeric fluid within the crack, acoustic emissions are emitted due to loss of the adhesive bond. To detect this debonding an external stress, such as through three- or four-point bending tests, is required for the application of the AE analysis to monitor the healing performance. In combination

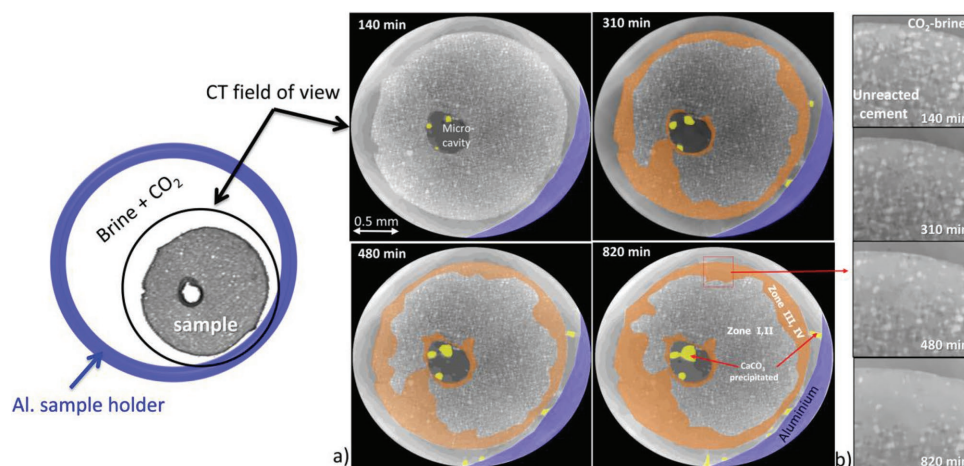


Figure 14. a) Cross-sections of the cement sample during the in situ CO₂-brine exposure. Zone I represents unreacted cement, II CH depleted zone, III fully carbonated zone, and IV porous zone depleted of calcium. The brighter zones (zones III and IV) in the slices are highlighted in orange for ease of visualization. The sketch to the left illustrates the off-axis position of the sample within the Al container. b) Zoomed-in view of a region of zones III and IV. Reproduced with permission.^[251] Copyright 2017, American Chemical Society.

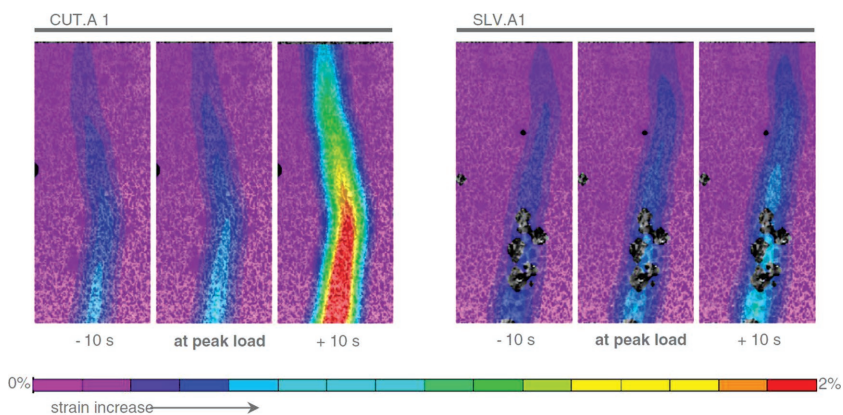


Figure 15. DIC monitoring of strain along the crack height at peak load and at snapshots taken 10 s before and after. Crack healing occurred through release of a rigid (CUT.A1) or a flexible (SLV.A1) polyurethane. Reproduced with permission.^[256] Copyright 2017, Elsevier.

with additional nondestructive testing methods such as DIC, ultrasonic testing (individual and continuous) vibration analysis, acoustic emission data can be correlated as in AE analysis for structural health monitoring (SHM), previously used damage parameters such as the (improved) b-value can be used to evaluate stress drops, stress redistribution and micro- or macrocrack behavior.^[257–260] A broad overview of the parameter-based evaluation of fatigue damaged reinforced cementitious materials is presented by Noorsuhada.^[257]

In **Figure 16**, a qualitative healing performance by locating released acoustic emission for autogenous healing (**Figure 16**, left) and for manual healing (**Figure 16**, right) is presented. Microcracks in the concrete specimens were partially filled by a two-component epoxy resin via embedded glass capillaries. The rapid reaction between the two epoxy components prevented a more extensive spread into the cracks. Fluorescent particles were added to the precursor to reveal the area of propagation of the epoxy resin. By locating emerging high-energy emissions while loading the beam 7 d after the initial crack formation, the epoxy resin failure correlates for the manual healing with the localization results perfectly. For the specimen repaired by autogenous healing, additional mismatching acoustic emissions are recorded. Supplementary parameter-based evaluation methods did not provide any further insight to their origin.

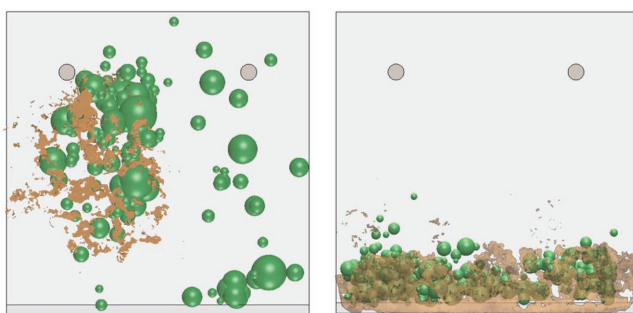


Figure 16. Results of the acoustic emission analysis of reinforced concrete beams (550 × 150 × 150 mm) with autonomous (left) and manual (right) healing properties. Green dots mark the localized acoustic emissions after reloading. Additionally, brown areas mark the distribution of epoxy precursors.

Further studies have also proven that a generalization on the applicability of evaluation methods for cementitious materials repaired by polymers cannot be made.^[158,256] Individual factors such as type of sensors, material composition, amplification technology, load scenario, etc., as well as the healing procedure (type of healing agents, manual or autogenous healing, encapsulation method, number and distribution of healing agents) individualize each test series.

Most of the aforementioned NDT techniques are focused or limited to characterizing individual phenomena such as local damage, the fluid propagation behavior of different polymers, or crack sealing behavior. In contrast, vibration analysis can be used to characterize and compare the entire system

without damaging the specimen. This property enables the technique to be used for evaluating the healing performance of force-fitting polymers and resins. The different states (initial, cracked, healed) to be investigated can be distinguished by their harmonic resonance vibration. The dynamic Young's modulus or shear modulus may be determined by a conversion of the individual resonance frequency from the fundamental mode. Since reinforced concrete or mortar test specimens are composite materials, it is not possible to make a qualitative assessment of the degree of damage. The same applies to the assessment of healing efficiency for mechanical properties. Due to the resulting novel cementitious composite containing additional bonding (healing) materials, it may be possible to exceed the initial, uncracked stiffness. This has already been proven by using the load-CMOD (crack mouth open displacement) curve.^[162]

7.3. Other Methods to Study the Healing Performance

Yildirim et al.^[261] evaluated the self-healing performance of cementitious composites with three different nondestructive testing methods namely: electrical impedance (EI) testing using a concrete resistivity meter, a rapid chloride permeability test (RCPT) measuring the current passing through a sample being exposed to a NaCl solution at one side and a NaOH solution at the other sample side while current is applied across the two opposite sides and resonant frequency (RF) analysis using steel balls to generate impact and thin-end pick-up sensors for detection. It was concluded that EI testing could prove the occurrence of self-healing, while for RCPT and RF test results, self-healing was less clearly noticed. As EI is easy to perform and takes limited time, this nondestructive testing method seems promising for self-healing assessment. However, it should be noticed that EI is very sensitive for changes in the ionic state of the specimen. When comparing each of the three techniques, a clear exponential relationship was found between EI and RCPT measurements. Results from RF did not seem to correlate with EI and RCPT due to the fact that different parameters affect each of these test results. While EI and RCPT are mostly influenced by the pore conditions (size, discontinuity

and tortuosity, or pore network) and the chemical composition of the pore fluid, RF is mainly influenced by changes in dynamic modulus of elasticity and mechanical integrity. Only when changes in the parameters effecting EI and RCPT also considerably improve the mechanical properties of the material, it will be detected by RF.

The healing performance may also be studied by means of nuclear magnetic resonance (NMR) tests.^[262] In this specific publication, a glass tube is embedded in a specimen. After cracking the specimen, it was glued and sealed at the exterior. Using a syringe, extra water was added in the glass tube, thus inducing autogenous healing. NMR was quantitatively used to study the water profiles.^[145] By comparing the masses determined by means of a balance and by means of NMR, conclusions could be drawn on the extent of autogenous healing. The NMR signal decreased due to the decrease of the total porosity in the saturated region. A very slight increase of the NMR signal of gel pores suggested that additional gel had been formed in the bulk paste adjacent to the crack. The results were further substantiated by means of EDX measurements. A solid-state NMR (SS-NMR) and powder XRD may be combined to study the binding mechanism for self-healing cementitious materials and the assessment of the reactivity of the healing agent with the cementitious constituents.^[263]

8. Conclusions

During the development of a new construction material with self-healing abilities, it is essential to get as much information as possible about its performance. For example, nondestructive testing has the potential to evaluate fractures in concrete but also to monitor the release of healing agents or the loss and regain of properties including gas or water tightness. A selection of nondestructive and minimal invasive techniques has been presented in this review paper including spectroscopic methods as well as techniques based on classical NDT methods such as CT, ultrasound, vibration, and AE techniques.

For the in situ application of the self-healing material additional tasks, consisting of a proof of activation of the healing mechanism in larger components and the determination of the in situ healing efficiency, are required. A stakeholder would invest in such a new material only, if the effective operation of healing is verified. The presented methods cover the full scale from microscopic and mesoscopic material tests up to techniques that can proof the performance of self-healing in situ at a construction. It is not always easy to select the most useful NDT technique for example to detect the presence and geometry of cracks in concrete and in most cases, a combination of different techniques is required. However, the review paper

Table 1. Possibilities and characteristics studied, boundary conditions, advantages, and disadvantages of the nondestructive and minimal invasive testing techniques.

Nondestructive and minimal invasive testing technique	Possibilities and characteristics studied	Boundary conditions	Advantages	Disadvantages
Digital and/or stereo microscopic analysis	<ul style="list-style-type: none"> • Visual monitoring; • Performance of encapsulated healing agents and possible coatings; • Surface, size and size distribution of healing agents and products; • Fracture behavior of encapsulation materials; • Stability and durability of encapsulated materials; • Formation of healing products; • Distribution of healing agents; • Microstructural properties; • Crack closure, crack width and healing percentage. 	<ul style="list-style-type: none"> • Depending on the magnification used; • μm features. 	<ul style="list-style-type: none"> • Quick, easy and straightforward; • A time study of the healing rate is possible; • Can be combined with other techniques. 	<ul style="list-style-type: none"> • Resolution limited to wavelength light itself; • Larger samples are difficult to move; • No 3D information; • Sometimes drying is needed and may stimulate autogenous healing due to the presence of carbon dioxide; • Drying with compressed air is not advisable as formed crystals may loosen.
Digital image correlation (DIC)	<ul style="list-style-type: none"> • Detection of crack development, widening and closure; • Simultaneous information about the width of multiple cracks in a larger area. 	<ul style="list-style-type: none"> • Will depend on the camera resolution and the resolution of the speckle pattern; • μm features. 	<ul style="list-style-type: none"> • Recorded as a movie or images with regular time intervals. 	<ul style="list-style-type: none"> • Sensitivity to other light sources; • Need of applying a speckle pattern.
Scanning electron microscope (or SEI)	<ul style="list-style-type: none"> • Sample's surface topography, electrical conductivity; • Size and size distribution of healing agents and products; • Morphology, thickness, size, shape and shell surface of capsules; • Distribution of healing agents and pore formation; • Crack closure; • Hydration degree. 	<ul style="list-style-type: none"> • 0.1 nm features, details 1 to 5 nm in size. 	<ul style="list-style-type: none"> • High level of detail, complexity inaccessible by optical microscopy. 	<ul style="list-style-type: none"> • Samples need to be dry, coated with gold or carbon; Need for sample preparation; • No 3D information; • Limited space in the equipment and thus need for reduction in sample size.

Table 1. Continued.

Nondestructive and minimal invasive testing technique	Possibilities and characteristics studied	Boundary conditions	Advantages	Disadvantages
Back-scattered electron microscopy combined with SEM	<ul style="list-style-type: none"> • Elemental mapping of a sample; • Crystallization and formation of healing products. 	<ul style="list-style-type: none"> • 0.1 nm features, details 1 to 5 nm in size. 	<ul style="list-style-type: none"> • High level of detail, complexity inaccessible by optical microscopy. 	<ul style="list-style-type: none"> • Samples need to be dry, coated with gold or carbon; Need for sample preparation; • No 3D information; • Limited place in the equipment and thus need for reduction in sample size.
Energy-dispersive X-ray spectroscopy (or EDX) combined with SEM	<ul style="list-style-type: none"> • Elemental analysis, chemical characterization based on the atomic structure; • Crystallization and formation of healing products; • Crystal phases; • Composition of the sealing deposits. 	<ul style="list-style-type: none"> • 0.1 nm features, details 1 to 5 nm in size. 	<ul style="list-style-type: none"> • Point analysis, line scans and point mappings are possible. 	<ul style="list-style-type: none"> • Samples need to be dry, coated with gold or carbon; Need for sample preparation; • No 3D information; • Limited place in the equipment and thus need for reduction in sample size; • Knowledge on Rietveld analysis is required.
Lab-based X-ray tomography	<ul style="list-style-type: none"> • 3D information; • Monitor dynamic changes in real time both qualitatively and quantitatively; • Water movement; • Crystallization and formation of healing products; • Leakage properties and outflow; • Distribution of healing agents and pore formation; • Creation of cracks; • Crack closure; • Self-sealing and regain in impermeability; • Connected pore space and pore size distribution; • Pitting corrosion of rebars. 	<ul style="list-style-type: none"> • From several centimeters large specimens down to 1 mm • Resolution related to sample size; maximum temporal resolution on the order of 12 s per scan. 	<ul style="list-style-type: none"> • 3D information; • Nondestructive; • Highly accessible; • Gray values/X-ray attenuation related to average atomic number and density sample. 	<ul style="list-style-type: none"> • Higher resolution requires small samples; • Not ideal for materials with high atomic number.
Synchrotron tomography	<ul style="list-style-type: none"> • Similar like lab-based tomography 3D information. 	<ul style="list-style-type: none"> • Higher spatial and temporal resolution than lab-based tomography. 	<ul style="list-style-type: none"> • Ideal to monitor large amounts of samples or to image fast dynamic processes. 	<ul style="list-style-type: none"> • More limited in access; • Not widely available.
Neutron tomography	<ul style="list-style-type: none"> • 3D information; • Monitor dynamic changes in real time; • Visualization liquid movement. 	<ul style="list-style-type: none"> • Typical several centimeter; • Resolution on the order of 10 μm and above. 	<ul style="list-style-type: none"> • 3D information; • Neutrons interact with lower atomic numbers such as H; • Water in dense rocks and cementitious materials is seen with neutrons. 	<ul style="list-style-type: none"> • Not widely available; • Samples become radioactive.
Ultrasonic testing, acoustic techniques (general)	<ul style="list-style-type: none"> • Small changes in material microstructure; • Differences in composition, curing conditions, moisture content or microstructure effects; setting behavior; • Elastic material properties such as the dynamic modulus of elasticity. 	<ul style="list-style-type: none"> • Elastic waves with frequencies between 20 kHz and 10 MHz. 	<ul style="list-style-type: none"> • Can be applied in a continuous way; • Can be applied during testing other characteristics. 	<ul style="list-style-type: none"> • At frequencies where the wavelength and the internal feature are of the same order, waves are highly attenuated by scattering and dissipation; • Noise needs to be filtered; • Reproducible measurement procedure is essential to obtain a quantified result.
Surface coupled transmission measurements	<ul style="list-style-type: none"> • Quantitative crack depth and crack healing (polymer-based) measurements by ultrapulse velocity measurements; • Differences in microstructure, qualitative crack closure (healing) validation by parameter- (e.g., amplitude, energy) and signal-based (e.g., diffusivity) analysis. 	<ul style="list-style-type: none"> • Accessibility to the structure; • Evaluation method depends on free accessible coupling surface. 	<ul style="list-style-type: none"> • Static and continuous measurements; • Applicable to existing structures – focusing on relevant areas. 	<ul style="list-style-type: none"> • Reproducible coupling: same transducers and sensor placement; • Surface (sensor placement) must be clean and smooth.

Table 1. Continued.

Nondestructive and minimal invasive testing technique	Possibilities and characteristics studied	Boundary conditions	Advantages	Disadvantages
Embedded sensors (Smart aggregates – SMAGs)	<ul style="list-style-type: none"> • Qualitative crack closure (healing) validation by parameter- (e.g., amplitude, energy) and signal-based (e.g., diffusivity) analysis. 			<ul style="list-style-type: none"> • Applicability only to new structures; • Areas to be examined must be known in advance; • Compound between sensor and surrounded material cannot be validated; • Up to now: low-budget quality.
Coda wave interferometry (CWI)	<ul style="list-style-type: none"> • Monitoring weak changes by acoustic elastic effect; • Detecting global stress changes, microcracking, global crack filling. 	<ul style="list-style-type: none"> • Control of all relevant impacts necessary (due to high sensitivity). 	<ul style="list-style-type: none"> • High sensitivity to weak perturbations in cementitious materials; • Improvement by low-frequency modulations; • (On-site) applicability to real structures. 	<ul style="list-style-type: none"> • Detects relative velocity changes: only global (averaged) characterization (up to now).
Acoustic emission	<ul style="list-style-type: none"> • Low signal amplitude compared to ultrasonic methods; • Spatial crack propagation in both the outer and the inner regions of structures in real time; • Recording the activation of capsule rupture or fracture of a building material; • Crack initiation and crack propagation. 	<ul style="list-style-type: none"> • Frequency range between 20 and 100 kHz; • Possible to localize events in $150 \times 250 \times 3000 \text{ mm}^3$ samples. 	<ul style="list-style-type: none"> • Different algorithms are available; • Different energy events for crack formation and capsule breakage or other features. 	<ul style="list-style-type: none"> • Comparison between different individual experiments and setups is difficult; • Strongly depends on the accuracy of the localization. In order to increase the reliability a large number of sensors are necessary; • Increased dimensions localization more complex and method becomes more limited; • Detailed description of the test procedure is necessary; • Reproducible measurement procedure is essential to obtain a quantified result; • Sensitive to environmental noises; • Requires high signal quality.
Contact angle measurements	<ul style="list-style-type: none"> • Curvature of a fluid interface; • Release efficiency; • Surface energy; • Change in surface property such as high hydrophobicity or hydrophilicity. 	<ul style="list-style-type: none"> • Depending of the surface properties. 	<ul style="list-style-type: none"> • Can be combined with microscopic analysis, SEM and micro-CT. 	<ul style="list-style-type: none"> • Required fluid may influence the hydration properties.
X-ray diffraction	<ul style="list-style-type: none"> • Constituents of crystalline healing agents and products. 	<ul style="list-style-type: none"> • Powder sample, several mg. 	<ul style="list-style-type: none"> • Databases with different crystallography information are available. 	<ul style="list-style-type: none"> • Only crystalline materials can be analyzed; • Knowledge on Rietveld analysis is required.
Thermogravimetric analysis	<ul style="list-style-type: none"> • Constituents of healing agents and products; • Verification of degradation upon increase in temperature. 	<ul style="list-style-type: none"> • Powder sample, several mg. 	<ul style="list-style-type: none"> • Widely used test; • Quantitative measurements. 	<ul style="list-style-type: none"> • Use of a powder; • Sample is heated; • Gases may form.
Differential scanning calorimetry	<ul style="list-style-type: none"> • Fusion and crystallization events; • Glass transition temperature. 	<ul style="list-style-type: none"> • Powder sample, several mg. 	<ul style="list-style-type: none"> • Combined with TGA. 	<ul style="list-style-type: none"> • Small powder sample.
Electron probe microanalysis (EMPA)	<ul style="list-style-type: none"> • Technique similar to SEM-EDX and analogous to Raman spectroscopy; • Composition of the studied material. 	<ul style="list-style-type: none"> • μm features. 	<ul style="list-style-type: none"> • See SEM-EDX. 	<ul style="list-style-type: none"> • See SEM-EDX.
Fourier transform infrared spectroscopy	<ul style="list-style-type: none"> • Absorbed or emitted light in a material in a wide spectral range; • Composition of the material. 	<ul style="list-style-type: none"> • Reflectance in micrometer range. 	<ul style="list-style-type: none"> • Can be combined with other techniques. 	<ul style="list-style-type: none"> • Small powder sample needed.

Table 1. Continued.

Nondestructive and minimal invasive testing technique	Possibilities and characteristics studied	Boundary conditions	Advantages	Disadvantages
Water permeability test and water leakage test	<ul style="list-style-type: none"> • Water permeability; • Recovery of water-tightness. 	<ul style="list-style-type: none"> • Depending on the sample size. 	<ul style="list-style-type: none"> • Gluing a water basin on top of a large specimen gives an idea about the sealing efficiency if cracks are not interconnected. 	<ul style="list-style-type: none"> • Water may stimulate autogenous healing and may alter the hydration degree; • Sometimes need to drill cores. • Precautions should be made for a good adhesion of the test setup to the overall material as leaks should be avoided; • Not possible to be used when neighboring cracks are interconnected.
Capillary water absorption test	<ul style="list-style-type: none"> • Water movement at distinct locations; • Rate of moisture diffusion; • Degree of capillary water uptake. 	<ul style="list-style-type: none"> • Depending on the sample size. 	<ul style="list-style-type: none"> • Can be combined with X-ray and/or neutron radiography. 	<ul style="list-style-type: none"> • Water may stimulate autogenous healing and may alter the hydration degree.
3D thermal distribution and infrared thermal imaging	<ul style="list-style-type: none"> • Increases in temperature and thermal distribution. 	<ul style="list-style-type: none"> • μm–mm features. 	<ul style="list-style-type: none"> • Easy verification of the healing performance when self-healing mechanisms containing heating devices or heating are studied. 	<ul style="list-style-type: none"> • Less useful for self-healing mechanisms without heating.
Electrical impedance	<ul style="list-style-type: none"> • Concrete resistivity meter; • Changes in dynamic modulus of elasticity. 	<ul style="list-style-type: none"> • Depending on the sample size. 	<ul style="list-style-type: none"> • Quick. 	<ul style="list-style-type: none"> • Not widely used to study self-healing; • Not for large specimens.
Nuclear magnetic resonance	<ul style="list-style-type: none"> • Quantitative and qualitative study of the water profiles; • Linked to the pore (gel) structure. 	<ul style="list-style-type: none"> • nm features. 	<ul style="list-style-type: none"> • Very detailed study as a function of time. 	<ul style="list-style-type: none"> • Not widely available; • Not for large specimens.

provides an overview about the state-of-the-art in this field and certainly helps to make the most appropriate selection.

In this review paper, different nondestructive techniques were analyzed in terms of their application to study self-healing in building materials. Due to the huge progress and development of different nondestructive and minimal invasive research techniques, new possibilities to study self-healing of materials are open. They offer valuable new insights and when combined they result in crucial insights in the characteristics and dynamics of a self-healing system. Depending on the stage of the investigation, several techniques have proven to be useful and will certainly be used in future studies.

Table 1 shows a summary of the different nondestructive and minimal invasive testing techniques, with their possible application, an overview of the characteristics that may be studied, their boundary conditions, and advantages and disadvantages.

Supporting Information

Supporting Information is available from the Wiley Online Library or from the author.

Acknowledgements

Some parts of the described experiments were financially supported by the European Commission in the 7th Framework Programme under the

acronym HealCon. The support of all HealCon partners during the project is gratefully acknowledged. As a Postdoctoral Research Fellow of the Research Foundation-Flanders (FWO-Vlaanderen), D. Snoeck would like to thank the foundation for the financial support (12J3617N). The authors from Technical University of Munich are indebted for significant help by Rudolph Kraus, Marina Nahm, Kathrin Flohr, and Gergana Maznikova.

Conflict of Interest

The authors declare no conflict of interest.

Keywords

2D and 3D characterization, digital imaging, nondestructive testing, property analysis, self-healing

Received: January 31, 2018
Revised: March 6, 2018
Published online: June 7, 2018

- [1] A. Mignon, D. Snoeck, P. Dubruel, S. Van Vlierberghe, N. De Belie, *Materials* **2017**, *10*, E237.
- [2] F. O. Anderegg, *ASTM Bull.* **1942**, *16*.
- [3] R. K. Dhir, C. M. Sangha, J. G. L. Munday, *J. Am. Concr. Inst.* **1973**, *70*, 231.
- [4] V. Mechtcherine, C. Schröfl, M. Wyrzykowski, M. Gorges, D. Cusson, J. Margeson, N. De Belie, D. Snoeck, K. Ichimiya,

- S.-I. Igarashi, V. Falikman, S. Friedrich, J. Bokern, P. Kara, P. Lura, A. Marciniak, H.-W. Reinhardt, S. Sippel, A. B. Ribeiro, J. Custódio, G. Ye, H. Dong, J. Weiss, *Mater. Struct.* **2017**, 50, 1.
- [5] S. Jacobsen, E. J. Sellevold, *Cem. Concr. Res.* **1996**, 26, 55.
- [6] K. Van Tittelboom, N. De Belie, *Materials* **2013**, 6, 2182.
- [7] B. Lubelli, T. G. Nijland, R. P. Van Hees, *Heron* **2011**, 56, 76.
- [8] D. Snoeck, N. De Belie, *Constr. Build. Mater.* **2015**, 95, 774.
- [9] N. ter Heide, in *Civil Engineering and Geosciences, Microlab*, Delft University of Technology, Delft, The Netherlands **2005**, p. 128.
- [10] S. Granger, A. Loukili, G. Pijaudier-Cabot, G. Chanvillard, *Cem. Concr. Res.* **2007**, 37, 519.
- [11] C. Edvardsen, *ACI Mater. J.* **1999**, 96, 448.
- [12] C. Joseph, D. Gardner, T. Jefferson, B. Isaacs, B. Lark, *Constr. Mater.* **2011**, 164, 29.
- [13] N. Z. Muhammad, A. Shafaghat, A. Heyvanfar, M. Z. Abd Majid, S. K. Ghoshal, S. E. M. Yasouj, A. A. Ganiyu, M. S. Kouchaksaraei, H. Kamyab, M. M. Taheri, M. R. Shirdar, R. McCaffer, *Constr. Build. Mater.* **2016**, 112, 1123.
- [14] A. Talaiekhozan, A. Keyvanfar, A. Shafaghat, R. Andalib, M. Z. Abd Majid, M. A. Fulazzaky, R. M. Zin, C. T. Lee, M. W. Hussin, N. Hamzah, N. F. Marwar, H. I. Haidar, *J. Environ. Treat. Tech.* **2014**, 2, 1.
- [15] W. Tang, O. Kardani, H. Cui, *Constr. Build. Mater.* **2015**, 81, 233.
- [16] M. Wu, B. Johannesson, M. Geiker, *Constr. Build. Mater.* **2012**, 28, 571.
- [17] H. W. Reinhardt, M. Jooss, *Cem. Concr. Res.* **2003**, 33, 981.
- [18] A. Neville, *Concr. Int.* **2002**, 24, 76.
- [19] N. Hearn, *Mater. Struct.* **1998**, 31, 563.
- [20] O. Çopuroglu, E. Schlangen, T. Nishiwaki, K. Van Tittelboom, D. Snoeck, N. De Belie, M. R. de Rooij, in *Self-Healing Phenomena in Cement-Based Materials: State-of-the-Art Report of RILEM Technical Committee 221-SHC*, Vol. 11 (Eds: M. R. de Rooij, K. Van Tittelboom, N. DeBelie, E. Schlangen), Springer, New York **2013**.
- [21] D. Józwiak-Niedźwiedzka, *Microsc. Res. Tech.* **2014**, 78, 22.
- [22] D. Snoeck, N. De Belie, *J. Mater. Civ. Eng.* **2015**, 04015086, 1.
- [23] S. Jacobsen, J. Marchand, H. Hornain, *Cem. Concr. Res.* **1995**, 25, 55.
- [24] K. L. Scrivener, *Cem. Concr. Comps.* **2004**, 26, 935.
- [25] R. Snellings, M. De Schepper, K. De Buysser, I. Van Driessche, N. De Belie, *J. Am. Ceram. Soc.* **2012**, 95, 1741.
- [26] V. Cnudde, M. Boone, *Earth Environ. Sci.* **2013**, 123, 1.
- [27] A. Stefánsson, I. Gunnarsson, N. Giroud, *Anal. Chim. Acta* **2007**, 582, 69.
- [28] K. Aki, P. G. Richards, *Quantitative Seismology*, University Science Books, Sausalito, CA **1980**.
- [29] W. M. Telford, L. P. Geldart, R. E. Sheriff, *Applied Geophysics*, Cambridge University Press, Cambridge **1990**.
- [30] P. Shearer, *Introduction to Seismology*, Cambridge University Press, Cambridge **1999**.
- [31] C. U. Große, in *Fakultät für Bauingenieur- und Vermessungswese*, Universität Stuttgart, Stuttgart, Germany **1996**.
- [32] C. Sens-Schönfelder, J. Ritter, U. Wegler, C. U. Grosse, presented at Noise and Diffuse Wavefields – Extended Abstracts of the Neustadt Workshop, *Conf. Deutschen Geophysikalischen Gesellschaft; Sonderband II*, Neustadt a. d. Weinstrasse, Germany, July **2009**, p. 133.
- [33] K. F. Bompan, V. G. Haach, *Constr. Build. Mater.* **2018**, 162, 740.
- [34] V. G. Haach, F. C. Ramirez, *Constr. Build. Mater.* **2016**, 119, 61.
- [35] M. Benaicha, O. Jalbaud, A. H. Alaoui, Y. Burtshell, *Constr. Build. Mater.* **2015**, 101, 702.
- [36] V. Pfister, A. Tundo, V. A. M. Luprano, *Constr. Build. Mater.* **2014**, 61, 278.
- [37] F. Benmeddour, G. Villain, O. Abraham, M. Choinska, *Constr. Build. Mater.* **2012**, 37, 934.
- [38] A. Van Hauwaert, J.-F. Thimus, F. Delannay, *Ultrasonics* **1998**, 36, 209.
- [39] P. Fröjd, P. Ulriksen, *NDT&E Int.* **2016**, 77, 35.
- [40] G. Kim, J.-Y. Kim, K. E. Kurtis, L. J. Jacobs, *Cem. Concr. Res.* **2017**, 92, 16.
- [41] C.-W. In, R. B. Holland, J.-Y. Kim, K. E. Kurtis, L. F. Kahn, L. J. Jacobs, *NDT&E Int.* **2013**, 57, 36.
- [42] W. Punuraj, J. Jarzynski, K. E. Kurtis, L. J. Jacobs, *Mech. Res. Commun.* **2007**, 34, 289.
- [43] M. Seher, C.-W. In, J.-Y. Kim, K. E. Kurtis, L. J. Jacobs, *J. Non-destruct. Eval.* **2013**, 22, 81.
- [44] A. Quiviger, C. Payan, J.-F. Chaix, V. Garnier, J. Salin, *NDT&E Int.* **2012**, 45, 128.
- [45] B. Hilloulin, J.-B. Legland, E. Lys, O. Abraham, A. Loukili, F. Grondin, O. Durand, V. Tournat, *Constr. Build. Mater.* **2016**, 123, 143.
- [46] B. Hilloulin, Y. Zhang, O. Abraham, A. Loukili, F. Grondin, F. Durand, V. Tournat, *NDT&E Int.* **2014**, 68, 98.
- [47] D. P. Schurr, in *School of Civil and Environmental Engineering*, Georgia Institute of Technology, Atlanta, GA **2010**, p. 119.
- [48] P. Fröjd, P. Ulriksen, *Ultrasonics* **2017**, 80, 1.
- [49] Y. Lu, J. E. Michaels, *Ultrasonics* **2005**, 43, 717.
- [50] F. Deroo, J.-Y. Kim, J. Qu, K. Sabra, L. J. Jacobs, *J. Acoust. Soc. Am.* **2010**, 127, 3315.
- [51] M. F. Cosmes-López, F. Castellanos, P. F. d. J. Cano-Barrita, *Ultrasonics* **2017**, 73, 88.
- [52] F. Puente León, *Messtechnik*, KIT Scientific Publishing Karlsruhe, Germany **2012**.
- [53] A. V. Oppenheim, R. W. Schaffer, *Discrete-Time Signal Processing*, Prentice-Hall, NJ **2013**.
- [54] M. Ohtsu, *Acoustic Emission (AE) and Related Non-destructive Evaluation (NDE) Techniques in the Fracture Mechanics of Concrete: Fundamentals and Applications*, Woodhead Publishing, Cambridge **2015**.
- [55] N. Robeyst, C. U. Grosse, N. De Belie, *Cem. Concr. Res.* **2009**, 39, 868.
- [56] N. Robeyst, E. Gruyaert, C. U. Grosse, N. De Belie, *Cem. Concr. Res.* **2008**, 38, 1169.
- [57] H. K. Lee, K. M. Lee, Y. H. Kim, H. Yim, D. B. Bae, *Cem. Concr. Res.* **2004**, 34, 631.
- [58] H. W. Reinhardt, C. U. Große, A. Herb, *Mater. Struct.* **2000**, 33, 580.
- [59] J. H. Kurz, C. U. Große, H. W. Reinhardt, *Ultrasonics* **2005**, 43, 538.
- [60] J. Carette, S. Staquet, *Cem. Concr. Comps.* **2016**, 73, 1.
- [61] *Advanced Testing of Cement-Based Materials During Setting And Hardening*, RILEM Report (Eds: H.-W. Reinhardt, C. U. Grosse), RILEM Publications SARL, Cachan, France **2005**, p. 341.
- [62] G. Karaiskos, A. Deraemaeker, D. G. Aggelis, D. Van Hemelrijck, *Smart Mater. Struct.* **2015**, 24, 113001.
- [63] C. U. Grosse, D. Aggelis, T. Shiotani, *Concrete Structures* (Ed: M. Ohtsu), Springer, Berlin **2016**, p. 5.
- [64] W. Liang, P. Que, *Measurement* **2009**, 42, 164.
- [65] B. Wu, Y. Huang, S. Krishnaswamy, *NDT&E Int.* **2017**, 85, 76.
- [66] N. Ruiz-Reyes, P. Vera-Candeas, J. Curpián-Alonso, R. Mata-Campos, J. C. Cuevas-Martínez, *NDT&E Int.* **2005**, 38, 453.
- [67] K. Xiao, Q. Wang, D. Hu, *Proc. Eng.* **2012**, 43, 419.
- [68] E. Ahn, H. Kim, S. H. Sim, S. W. Shin, M. Shin, *Materials* **2017**, 10, E278.
- [69] B. Weiler, C. U. Große, *Otto Graf J.* **1995**, 6, 1.
- [70] L. Brunarski, *Mater. Struct.* **1969**, 2, 269.
- [71] K. Subramaniam, J. Popovics, S. Shah, *Cem., Concr., Aggregates* **2000**, 22, 81.
- [72] B. J. Lee, S.-H. Kee, T. Oh, Y.-Y. Kim, *Adv. Mater. Sci. Eng.* **2015**, 580638, 1.
- [73] K. Jurowski, S. Grzeszczyk, *Proc. Eng.* **2015**, 108, 584.
- [74] R. Aguilar, E. Ramírez, V. G. Haach, M. A. Pando, *Constr. Build. Mater.* **2016**, 104, 181.
- [75] K. J. Leśnicki, J.-Y. Kim, K. E. Kurtis, L. J. Jacobs, *NDT&E Int.* **2011**, 44, 721.

- [76] C. U. Grosse, H.-W. Reinhardt, F. Finck, *J. Mater. Civ. Eng.* **2003**, 15, 274.
- [77] C. U. Grosse, M. Ohtsu, *Acoustic Emission Testing*, Springer-Verlag, Berlin **2008**.
- [78] S. Bancroft, *IEEE Trans. Aerosp. Electron. Syst.* **1985**, AES-21, 56.
- [79] J. H. Kurz, *Ultrasonics* **2015**, 63, 155.
- [80] S. Gollob, G. K. Kocur, T. Schumacher, L. Mhamdi, T. Vogel, *Ultrasonics* **2017**, 74.
- [81] S. Chen, C. Yang, G. Wang, W. Liu, *Ultrasonics* **2017**, 75, 36.
- [82] Z. Zhou, J. Zhou, L. Dong, X. Cai, Y. Rui, C. Ke, *Sci. Rep.* **2017**, 7, 7472.
- [83] G. Yan, J. Tang, *Math. Probl. Eng.* **2015**, 247839, 1.
- [84] A. Ebrahimkhanlou, S. Salamone, *Smart Mater. Struct.* **2017**, 26, 095026.
- [85] T. Kundu, *Ultrasonics* **2013**, 54, 25.
- [86] D. Snoeck, K. Van Tittelboom, S. Steuperaert, P. Dubruel, N. De Belie, *J. Intell. Mater. Syst. Struct.* **2014**, 25, 13.
- [87] D. Snoeck, D. Schaubroeck, P. Dubruel, N. De Belie, *Constr. Build. Mater.* **2014**, 72, 148.
- [88] M. T. Hasholt, O. M. Jensen, K. Kovler, S. Zhutovsky, *Constr. Build. Mater.* **2012**, 31, 226.
- [89] E. Gruyaert, B. Debbaut, D. Snoeck, P. Díaz, A. Arizo, E. Tziviloglou, E. Schlangen, N. De Belie, *Smart Mater. Struct.* **2016**, 25, 084007.
- [90] A. Mignon, G.-J. Graulus, D. Snoeck, J. Martins, N. De Belie, P. Dubruel, S. Van Vlierberghe, *J. Mater. Sci.* **2015**, 50, 970.
- [91] A. Mignon, D. Snoeck, D. Schaubroeck, N. Luickx, P. Dubruel, S. Van Vlierberghe, N. De Belie, *React. Funct. Polym.* **2015**, 93, 68.
- [92] J. Pelto, M. Leivo, E. Gruyaert, B. Debbaut, D. Snoeck, N. De Belie, *Smart Mater. Struct.* **2017**, 26, 1.
- [93] J. Wang, H. Soens, W. Verstraete, N. De Belie, *Cem. Concr. Res.* **2014**, 56, 139.
- [94] R. T. Armstrong, M. L. Porter, D. Wildenschild, *Adv. Water Res.* **2012**, 46, 55.
- [95] M. G. Andrew, B. Bijeljic, M. J. Blunt, *Adv. Water Res.* **2014**, 68, 24.
- [96] J. Schmatz, J. L. Urai, S. Berg, H. Ott, *Geophys. Res. Lett.* **2015**, 42, 2189.
- [97] K. A. Klise, D. Moriarty, H. Yoon, Z. Karpyn, *Adv. Water Res.* **2016**, 95, 152.
- [98] N. A. Idowu, M. J. Blunt, *Transp. Porous Media* **2010**, 83, 151.
- [99] K. Van Tittelboom, in *Structural Engineering and Architecture*, Ghent University, Ghent **2012**, p. 344.
- [100] Y.-K. Song, Y.-H. Jo, Y.-J. Lim, S.-Y. Cho, H.-C. Yu, B.-C. Ryu, S.-I. Lee, C.-M. Chung, *ACS Appl. Mater. Interfaces* **2013**, 5, 1378.
- [101] B. Dong, W. Ding, S. Qin, N. Han, G. Fang, Y. Liu, F. Xing, S. Hong, *Cem. Concr. Comps.* **2018**, 85, 83.
- [102] B. Dong, G. Fang, W. Ding, Y. Liu, J. Zhang, N. Han, F. Xing, *Constr. Build. Mater.* **2016**, 106, 608.
- [103] L. Lv, Z. Yang, G. Chen, G. Zhu, N. Han, E. Schlangen, F. Xing, *Constr. Build. Mater.* **2016**, 105, 487.
- [104] J.-F. Su, S. Han, Y.-Y. Wang, E. Schlangen, N.-X. Han, B. Liu, X.-L. Zhang, P. Yang, W. Li, *Constr. Build. Mater.* **2017**, 147, 533.
- [105] L. Y. Lv, E. Schlangen, Z. X. Yang, F. Xing, *Materials* **2016**, 9, E1025.
- [106] L. Liao, W. Zhang, Y. Xin, H. Wang, Y. Zhao, W. Li, *Chin. Sci. Bull.* **2011**, 56, 439.
- [107] J.-F. Su, P. Yang, Y.-Y. Wang, S. Han, N.-X. Han, W. Li, *Materials* **2016**, 9, 600.
- [108] B. Dong, N. Han, M. Zhang, X. Wang, H. Cui, F. Xing, *J. Earthquake Tsunami* **2013**, 7, 1.
- [109] E. Mostavi, S. Asadi, M. M. Hassan, M. Alansari, *J. Mater. Civ. Eng.* **2015**, 27, 4015035.
- [110] A. Kanellopoulos, P. Giannaros, A. Al-Tabbaa, *Constr. Build. Mater.* **2016**, 122, 577.
- [111] A. Kanellopoulos, P. Giannaros, A. Al-Tabbaa, *Smart Mater. Struct.* **2016**, 26, 45025.
- [112] P. Giannaros, A. Kanellopoulos, A. Al-Tabbaa, *Smart Mater. Struct.* **2016**, 25, 084005.
- [113] C. Dry, *Compos. Struct.* **1996**, 35, 263.
- [114] W. Li, Z. Jiang, Z. Yang, N. Zhao, W. Yuan, *PLoS One* **2013**, 8, 1.
- [115] T.-H. Ahn, T. Kishi, *J. Adv. Concr. Technol.* **2010**, 8, 171.
- [116] Y.-S. Lee, J.-S. Ryou, *Constr. Build. Mater.* **2014**, 71, 188.
- [117] Y. Yang, M. D. Lepech, E.-H. Yang, V. C. Li, *Cem. Concr. Res.* **2009**, 39, 382.
- [118] V. C. Li, in *Concrete Construction Engineering Handbook* (Ed: E. Nawy), CRC Press, Boca Raton, FL **2008**, p. 78.
- [119] V. C. Li, S. Wang, C. Wu, *ACI Mater. J.* **1997**, 98, 483.
- [120] V. C. Li, C. Wu, S. Wang, A. Ogawa, T. Saito, *ACI Mater. J.* **2002**, 99, 463.
- [121] D. Homma, H. Mihashi, T. Nishiwaki, *J. Adv. Concr. Technol.* **2009**, 7, 217.
- [122] D. Snoeck, in *Structural Engineering*, Doctor in Civil Engineering: Construction Design, Ghent University, Ghent **2015**, p. 364.
- [123] D. Snoeck, J. Dewanckele, V. Cnudde, N. De Belie, *Cem. Concr. Comps.* **2016**, 65, 83.
- [124] D. Snoeck, S. Steuperaert, K. Van Tittelboom, P. Dubruel, N. De Belie, *Cem. Concr. Res.* **2012**, 42, 1113.
- [125] P. Lura, G. Ye, V. Cnudde, P. Jacobs, presented at Int. Conf. on Microstructure Related Durability of Cementitious Composites, Nanjing, China, October **2008**.
- [126] H. Chen, C. Qian, H. Huang, *Constr. Build. Mater.* **2016**, 126, 297.
- [127] H. M. Jonkers, A. Thijssen, G. Muzzer, O. Çopuroğlu, E. Schlangen, *Ecol. Eng.* **2010**, 36, 230.
- [128] T. Nishiwaki, M. Koda, M. Yamada, H. Mihashi, T. Kikuta, *J. Adv. Concr. Technol.* **2012**, 10, 195.
- [129] D. Snoeck, N. De Belie, *Biosyst. Eng.* **2012**, 111, 325.
- [130] D. Snoeck, P.-A. Smetryns, N. De Belie, *Biosyst. Eng.* **2015**, 139, 87.
- [131] R. D. Tolêdo Filho, K. L. Scrivener, G. L. England, K. Ghavami, *Cem. Concr. Comps.* **2000**, 22, 127.
- [132] R. D. Tolêdo Filho, K. Ghavami, M. A. Sanjuán, G. L. England, *Cem. Concr. Comps.* **2005**, 27, 537.
- [133] P. Trtik, B. Muench, W. J. Weiss, G. Herth, A. Kaestner, E. Lehmann, P. Lura, presented at Int. RILEM Conf. on Material Science, Aachen, Germany, September **2010**.
- [134] C. Schröfl, D. Snoeck, V. Mechtcherine, *Mater. Struct.* **2017**, 50, 1.
- [135] D. Snoeck, O. M. Jensen, N. De Belie, *Cem. Concr. Res.* **2015**, 74, 59.
- [136] L. Ferrara, V. Krelani, M. Carsana, *Constr. Build. Mater.* **2014**, 68, 535.
- [137] Z. B. Bundur, A. Amiri, Y. G. Ersan, N. Boon, N. De Belie, *Cem. Concr. Res.* **2017**, 98, 44.
- [138] S.-W. Lee, M. Jo, J.-W. Kim, T. Kim, *Mater. Des.* **2016**, 89, 362.
- [139] W. De Muyneck, K. Cox, N. De Belie, W. Verstraete, *Constr. Build. Mater.* **2008**, 22, 875.
- [140] M. A. A. Sherif, K. M. A. Hossain, M. Lachemi, *Constr. Build. Mater.* **2016**, 127, 80.
- [141] J. Van Stappen, T. Bultreys, F. A. Gilabert Villegas, X. K. D. Hillewaere, D. Garoz Gómez, K. Van Tittelboom, J. Dhaene, N. De Belie, W. Van Paeppegem, F. Du Prez, V. Cnudde, *Mater. Charact.* **2016**, 119, 99.
- [142] F. A. Gilabert, K. Van Tittelboom, J. Van Stappen, V. Cnudde, N. De Belie, *Cem. Concr. Comps.* **2017**, 77, 68.
- [143] K. Van Tittelboom, J. Wang, M. A. Gomes De Araújo, D. Snoeck, E. Gruyaert, B. Debbaut, H. Derluyn, V. Cnudde, E. Tsangouri, D. Van Hemelrijck, N. De Belie, *Constr. Build. Mater.* **2016**, 108, 125.
- [144] Y. Yao, Y. Zhu, Y. Yang, *Constr. Build. Mater.* **2011**, 28, 139.
- [145] D. Snoeck, L. Pel, N. De Belie, *Sci. Rep.* **2017**, 7, 1.
- [146] D. Snoeck, L. F. Velasco, A. Mignon, S. Van Vlierberghe, P. Dubruel, P. Lodewyckx, N. De Belie, *Cem. Concr. Res.* **2015**, 77, 26.

- [147] K. Van Tittelboom, E. Tsangouri, D. Van Hemelrijck, N. De Belie, *Cem. Concr. Comps.* **2015**, 57, 142.
- [148] Á. García, E. Schlangen, M. van de Ven, Q. Liu, *Constr. Build. Mater.* **2009**, 23, 3175.
- [149] K. Van Tittelboom, N. De Belie, D. Van Loo, P. Jacobs, *Cem. Concr. Comps.* **2011**, 33, 497.
- [150] A. Kanellopoulos, T. S. Qureshi, A. Al-Tabbaa, *Constr. Build. Mater.* **2015**, 98, 780.
- [151] K. Van Tittelboom, D. Snoeck, P. Vontobel, F. H. Wittmann, N. De Belie, *Mater. Struct.* **2013**, 46, 105.
- [152] A. Formia, S. Irico, F. Bertola, F. Canonico, P. Antonaci, N. M. Pugno, J.-M. Tulliani, *J. Intell. Mater. Syst. Struct.* **2016**, 27, 2633.
- [153] B. Liu, J. L. Zhang, J. L. Ke, X. Deng, B. Q. Dong, N.-X. Han, F. Xing, presented at Int. Conf. on Self-Healing Materials, Durham, NC, June **2015**.
- [154] A. Danyuk, I. Rastegaev, E. Pomponi, M. Linderov, D. Merson, A. Vinogradov, *Proc. Eng.* **2017**, 176, 284.
- [155] G. K. Kocur, *J. Sound Vib.* **2017**, 387, 66.
- [156] E. Tsangouri, G. Karaiskos, D. Aggelis, A. Deraemaeker, D. Van Hemelrijck, *Struct. Health Monit.* **2015**, 14, 462.
- [157] E. Tsangouri, G. Karaiskos, A. Deraemaeker, D. Van Hemelrijck, D. Aggelis, *Constr. Build. Mater.* **2016**, 129, 163.
- [158] K. Van Tittelboom, N. De Belie, F. Lehmann, C. U. Grosse, *Constr. Build. Mater.* **2012**, 28, 333.
- [159] J. H. Kurz, S. Köppel, L. M. Linzer, B. Schechinger, C. U. Grosse, in *Acoustic Emission Testing: Basics for Research – Applications in Civil Engineering* (Eds: C. U. Grosse, M. Ohtsu), Springer, Berlin **2008**, p. 101.
- [160] M. Y. Bhuiyan, V. Giurgiutiu, *Materials* **2017**, 10, E962.
- [161] T. G. Nijland, J. A. Larbi, R. P. Van Hees, B. Lubelli, M. R. de Rooij, presented at Int. Conf. on Self Healing Materials, Noordwijk, The Netherlands, April **2007**.
- [162] B. Hilloulin, D. Hilloulin, F. Grondin, A. Loukili, N. De Belie, *Cem. Concr. Res.* **2016**, 80, 21.
- [163] K. Sisomphon, O. Çopuroğlu, E. A. B. Koenders, *Cem. Concr. Comps.* **2012**, 34, 566.
- [164] K. Van Tittelboom, E. Gruyaert, H. Rahier, N. De Belie, *Constr. Build. Mater.* **2012**, 37, 349.
- [165] M. Roig-Flores, F. Pirritano, P. Serna, L. Ferrara, *Constr. Build. Mater.* **2016**, 114, 447.
- [166] L. Ferrara, V. Krelani, F. Moretti, *Cem. Concr. Comps.* **2016**, 73, 299.
- [167] M. Roig-Flores, S. Moscato, P. Serna, L. Ferrara, *Constr. Build. Mater.* **2015**, 86, 1.
- [168] V. Achal, A. Mukherjee, D. Kumari, Q. Zhang, *Earth Sci. Rev.* **2015**, 148, 1.
- [169] V. Achal, A. Mukherjee, M. Sudhakar Reddy, *Constr. Build. Mater.* **2013**, 48, 1.
- [170] Y. C. Erşan, N. De Belie, N. Boon, *Biochem. Eng. J.* **2015**, 101, 108.
- [171] Y. C. Erşan, E. Gruyaert, G. Louis, C. Loris, N. De Belie, N. Boon, *Front. Microbiol.* **2015**, 6, 1.
- [172] Y. C. Erşan, E. Hernandez-Sanabria, N. Boon, N. De Belie, *Cem. Concr. Comps.* **2016**, 70, 159.
- [173] W. Khaliq, M. B. Ehsan, *Constr. Build. Mater.* **2016**, 102, 349.
- [174] H. M. Jonkers, *Heron* **2011**, 56, 1.
- [175] J. Wang, K. Van Tittelboom, N. De Belie, W. Verstraete, *Cem. Build. Mater.* **2012**, 26, 532.
- [176] S. Sangadji, V. Wiktor, H. M. Jonkers, E. Schlangen, *Proc. Eng.* **2017**, 171, 606.
- [177] L. Ferrara, presented at Int. RILEM Conf. on the Application of Superabsorbent Polymers and Other New Admixtures in Concrete Construction, Dresden, Germany, September **2014**.
- [178] L. Ferrara, V. Krelani, F. Moretti, M. Roig-Flores, P. Serna Ros, *Cem. Concr. Comps.* **2017**, 83, 76.
- [179] K. Olivier, A. Darquennes, F. Benboudjema, R. Gagné, *J. Adv. Concr. Technol.* **2016**, 14, 717.
- [180] M. Maes, D. Snoeck, N. De Belie, *Constr. Build. Mater.* **2016**, 115, 114.
- [181] V. C. Li, Y. M. Lim, Y. W. Chan, *Composites, Part B* **1988**, 29, 819.
- [182] M. Şahmaran, G. Yildirim, T. K. Erdem, *Cem. Concr. Comps.* **2013**, 35, 89.
- [183] G. Yildirim, M. Sahmaran, H. Ahmed, *J. Mater. Civ. Eng.* **2014**, 27, 04014187.
- [184] H. Mihashi, T. Nishiwaki, *J. Adv. Concr. Technol.* **2012**, 10, 170.
- [185] D. Palin, V. Wiktor, H. M. Jonkers, *Cem. Concr. Res.* **2015**, 73, 17.
- [186] S. Z. Qian, J. Zhou, M. R. de Rooij, E. Schlangen, G. Ye, K. van Breugel, *Cem. Concr. Comps.* **2009**, 31, 613.
- [187] T. S. Qureshi, A. Kanellopoulos, A. Al-Tabbaa, *Constr. Build. Mater.* **2016**, 121, 629.
- [188] J. Wang, A. Mignon, D. Snoeck, V. Wiktor, N. Boon, N. De Belie, *Front. Microbiol.* **2015**, 6, 1.
- [189] J. Wang, D. Snoeck, S. Van Vlierberghe, W. Verstraete, N. De Belie, *Constr. Build. Mater.* **2014**, 68, 110.
- [190] R. Alghamri, A. Kanellopoulos, A. Al-Tabbaa, *Constr. Build. Mater.* **2016**, 124, 910.
- [191] S. Sangadji, E. Schlangen, *J. Adv. Concr. Technol.* **2012**, 10, 185.
- [192] S. Sangadji, E. Schlangen, *Proc. Eng.* **2013**, 54, 315.
- [193] D. J. Kim, S. H. Kang, T.-H. Ahn, *Materials* **2014**, 7, 508.
- [194] C. Stuckrath, R. Serpell, L. M. Valenzuela, M. Lopez, *Cem. Concr. Comps.* **2014**, 50, 10.
- [195] J. Navarro-Gregori, E. J. Mezquida-Alcaraz, P. Serna-Ros, J. Echegaray-Oviedo, *Constr. Build. Mater.* **2016**, 112, 100.
- [196] B. Isaacs, R. Lark, T. Jefferson, R. Davies, S. Dunn, *Struct. Concr.* **2013**, 14, 138.
- [197] E. Tsangouri, G. Karaiskos, D. Aggelis, D. Van Hemelrijck, A. Deraemaeker, presented at 9th Int. Conf. on Structural Dynamic, Porto, Portugal, June–July **2014**.
- [198] H. M. Jonkers, in *Self Healing Materials. An Alternative Approach to 20 Centuries of Materials Science*, Vol. 100 (Ed: S. van der Zwaag), Springer, Berlin **2008**, p. 195.
- [199] J. Wang, in *Structural Engineering and Architecture*, Ghent University, Ghent **2013**, p. 303.
- [200] J. Wang, N. De Belie, W. Verstraete, *J. Ind. Microbiol. Biotechnol.* **2012**, 39, 567.
- [201] J. Xu, W. Yao, Z. Jiang, *J. Mater. Civ. Eng.* **2014**, 26, 983.
- [202] L. Kan, H. Shi, *Constr. Build. Mater.* **2012**, 29, 348.
- [203] L.-L. Kan, H.-S. Shi, A. R. Sakulich, V. C. Li, *ACI Mater. J.* **2010**, 107, 617.
- [204] S. Fan, M. Li, *Smart Mater. Struct.* **2015**, 24, 015021.
- [205] H. Huang, G. Ye, D. Damidot, *Cem. Concr. Res.* **2013**, 52, 71.
- [206] C. De Nardi, A. Cecchi, L. Ferrara, A. Benedetti, D. Cristofori, *Composites, Part B* **2017**, 124, 144.
- [207] G. Perez, J. J. Gaitero, E. Erkizia, I. Jimenez, A. Guerrero, *Cem. Concr. Comps.* **2015**, 60, 55.
- [208] D. Fukuda, M. Maruyama, Y. Nara, D. Hayashi, H. Ogawa, K. Kaneko, *Int. J. Fract.* **2014**, 188, 159.
- [209] C. De Nardi, S. Bullo, L. Ferrara, L. Ronchin, A. Vavasori, *Mater. Struct.* **2017**, 50, 1.
- [210] L. Lv, E. Schlangen, F. Xing, *Materials* **2017**, 10, 1.
- [211] T. Nishiwaki, H. Mihashi, B. K. Jang, K. Miura, *J. Adv. Concr. Technol.* **2006**, 4, 267.
- [212] Y. Sun, S. Wu, Q. Liu, W. Zeng, Z. Chen, Q. Ye, P. Pan, *Constr. Build. Mater.* **2017**, 150, 673.
- [213] A. Menozzi, Á. García, M. N. Partl, G. Tebaldi, P. Schuetz, *Constr. Build. Mater.* **2015**, 74, 162.
- [214] B. Van Belleghem, R. Montoya, J. Dewanckele, N. Van den Steen, I. De Graeve, J. Deconinck, V. Cnudde, K. Van Tittelboom, N. De Belie, *Constr. Build. Mater.* **2016**, 110, 154.

- [215] P. Van den Heede, B. Van Belleghem, N. M. Alderete, K. Van Tittelboom, N. De Belie, *Materials* **2016**, 9, 1.
- [216] J. Wang, J. Dewanckele, V. Cnudde, S. Van Vlierberghe, W. Verstraete, N. De Belie, *Cem. Concr. Comps.* **2014**, 53, 289.
- [217] G. Ganendra, J. Wang, J. A. Ramos, H. Derluyn, H. Rahier, V. Cnudde, A. Ho, N. Boon, *Front. Microbiol.* **2015**, 6, 1.
- [218] W. De Muynck, S. Leuridan, D. Van Loo, K. Verbeken, V. Cnudde, N. De Belie, W. Verstraete, *Appl. Environ. Microbiol.* **2011**, 77, 6808.
- [219] Á. García, J. Jelfs, C. J. Austing, *Constr. Build. Mater.* **2015**, 101, 309.
- [220] R. Micaelo, T. Al-Mansoori, Á. García, *Constr. Build. Mater.* **2016**, 123, 734.
- [221] D. Fukuda, Y. Nara, Y. Kobayashi, M. Maruyama, M. Koketsu, D. Hayashi, H. Ogawa, K. Kanedo, *Cem. Concr. Res.* **2012**, 42, 1494.
- [222] D. Fukuda, Y. Nara, D. Hayashi, H. Ogawa, K. Kaneko, *Materials* **2013**, 6, 2578.
- [223] T. Watanabe, Y. Fujiwara, C. Hashimoto, K. Ishimaru, *Int. J. Mod. Phys. B* **2011**, 25, 4307.
- [224] M. Henry, I. S. Darma, T. Sugiyama, *Constr. Build. Mater.* **2014**, 67, 37.
- [225] Q. Lv, W. Huang, X. Zhu, F. Xiao, *Mater. Des.* **2017**, 117, 7.
- [226] Á. García, *Fuel* **2012**, 93, 264.
- [227] C. Aldea, S. Shah, A. Karr, *J. Mater. Civ. Eng.* **1999**, 11, 181.
- [228] C. Aldea, W. Wong, J. S. Popovics, S. P. Shah, *J. Mater. Civ. Eng.* **2000**, 12, 92.
- [229] M. D. Lepech, V. C. Li, in *Proc. Int. Conf. on Fracture 11* (Ed: A. Carpinteri), Curran Associates, Inc, Red Hook, NY **2005**, p. 4539.
- [230] B. B. Sabir, S. Wild, M. O'Farrell, *Mater. Struct.* **1998**, 31, 568.
- [231] J. Feiteira, E. Gruyaert, N. De Belie, *Constr. Build. Mater.* **2016**, 102, 671.
- [232] R. Hassanein, *Ph.D. Thesis*, ETH Zurich, Zurich **2006**.
- [233] J. B. Molyneux, D. R. Schmitt, *Geophysics* **1999**, 64, 1492.
- [234] C. Hadziioannou, E. Larose, O. Coutant, P. Roux, M. Campillo, *J. Acoust. Soc. Am.* **2009**, 125, 3688.
- [235] T. Planès, E. Larose, *Cem. Concr. Res.* **2013**, 53, 248.
- [236] F. Malm, C. U. Grosse, presented at 19th World Conf. on Non-Destructive Testing, Muchen, Germany, June **2016**.
- [237] S. Granger, G. Pijaudier-Cabot, A. Loukili, D. Marlot, J. C. Lenain, *Cem. Concr. Res.* **2009**, 39, 296.
- [238] Y. Zhang, O. Abraham, A. Le Duff, B. Lascoup, V. Tournat, E. Larose, T. Planes, R. El Guerjouma, O. Durand, in *Nondestructive Testing of Materials and Structures*, (Eds: O. Güneş, Y. Akkaya), Springer, Dordrecht, The Netherlands **2013**, p. 233.
- [239] S. Thiele, J.-Y. Kim, J. Qu, L. J. Jacobs, *Ultrasonics* **2014**, 54, 1470.
- [240] S.-H. Kee, J. Zhu, *J. Acoust. Soc. Am.* **2010**, 147, 1279.
- [241] A. Spalvier, J. Bittner, S. K. Evani, J. S. Popovics, *AIP Conf. Proc.* **2017**, 1806, 080010.
- [242] G. Kim, C.-W. In, J.-Y. Kim, K. E. Kurtis, L. J. Jacobs, *NDT&E Int.* **2014**, 67, 64.
- [243] F. Schempp, J.-Y. Kim, *AIP Conf. Proc.* **2014**, 1581, 814.
- [244] L. Qin, S. Huan, X. Cheng, Y. Lu, Z. Li, *Smart Mater. Struct.* **2009**, 18, 095018.
- [245] C. Dumoulin, A. Deraemaeker, *Ultrasonics* **2017**, 79, 18.
- [246] D. G. Bekas, K. Tsirka, D. Baltzis, A. S. Paipetis, *Composites, Part B* **2016**, 87, 92.
- [247] M. A. Franesqui, J. Yepes, C. Carcía-González, *Constr. Build. Mater.* **2017**, 149, 612.
- [248] G. D. Quinn, J. J. Swab, *J. Am. Ceram. Soc.* **2000**, 83, 317.
- [249] H. Choi, J. S. Popovics, *IEEE Trans. Ultrason. Ferroelectr. Freq. Control* **2015**, 62, 1076.
- [250] K. Van Tittelboom, B. Van Belleghem, M. Boone, L. Van Hoorebeke, N. De Belie, *Adv. Mater. Interfaces* **2017**, 5, 1701021.
- [251] E. A. Chavez Panduro, M. Torsæter, K. Gawel, R. Bjerge, A. Gibaud, Y. Yang, S. Bruns, Y. Zheng, H. O. Sørensen, D. W. Breiby, *Environ. Sci. Technol.* **2017**, 51, 9344.
- [252] J. Van Stappen, in *Geology*, Ghent University, Ghent **2017**.
- [253] J. Van Stappen, T. De Kock, M. Boone, S. Olausson, V. Cnudde, *Norw. J. Geol.* **2014**, 94, 201.
- [254] M. G. Andrew, B. Bijeljic, M. J. Blunt, *Microsc. Anal.* **2014**, 28, S4.
- [255] P. Cao, K. Z. T. , L. Li, *Water Resour. Res.* **2015**, 51, 4684.
- [256] J. Feiteira, E. Tsangouri, E. Gruyaert, C. Lors, G. Louis, N. De Belie, *Mater. Des.* **2017**, 115, 238.
- [257] M. N. Noorsuhada, *Constr. Build. Mater.* **2016**, 112, 424.
- [258] R. Vidya Sagar, M. V. M. S. Rao, *Constr. Build. Mater.* **2014**, 70, 460.
- [259] M. E. Zitto, R. Piotrkowski, A. Gallego, F. Sagasta, A. Benavent-Climent, *Mech. Syst. Signal Process.* **2015**, 60, 75.
- [260] J. H. Kurz, F. Finck, C. U. Grosse, H.-W. Reinhardt, *Struct. Health Monit.* **2006**, 6, 69.
- [261] G. Yildirim, G. H. Aras, Q. S. Banyhussan, M. Şahmaran, M. Lachemi, *NDT&E Int.* **2015**, 76, 26.
- [262] H. Huang, G. Ye, L. Pel, *Mater. Struct.* **2016**, 1.
- [263] S. Irico, A. G. Bovio, G. Paul, E. Boccaleri, D. Gastaldi, L. Marchese, L. Buzzi, F. Canonico, *Cem. Concr. Comps.* **2017**, 76, 57.